Dalton Transactions

Accepted Manuscript

ROYAL SOCIETY OF CHEMISTRY

www.rsc.org/dalton

Relevant and Unprecedented C-H/σ Supramolecular Interactions Involving σ-Aromatic M_2X_2 Cores

Ashok Sasmal[a], Antonio Bauzá[b], Antonio Frontera[b], Corrado Rizzoli[c], Cédric Desplanches[d], Loïc J. Charbonnière[e], Samiran Mitra[a]*

[a]Department of Chemistry, Jadavpur University, Raja S.C. Mullick Road, Kolkata-700032, West Bengal, India.

[b]Departament de Química, Universitat de les Illes Balears, Crta. de Valldemossa km 7.5, 07122 Palma de Mallorca, Baleares, Spain.

[c]Universitá degli Studi di Parma, Dipartimento di Chimica, Parco Area delle Scienze 17/A I-43124 Parma, Italy.

[d]CNRS, Université de Bordeaux, ICMCB, 87 Avenue du Dr. A. Schweitzer, Pessac, F-33608, France

[e]Laboratoire d'Ingénierie Moléculaire Appliquée àl'Analyse, IPHC, UMR 7178 CNRS/UdS, ECPM Ba□t R1N0, 25 rue Becquerel, 67087 Strasbourg Cedex 2, France

* Corresponding author: Tel: + 91-33-2414 6666 (Extn. 2505); fax: + 91-33-2414 6414

E-mail address: samiranju92@gmail.com (Samiran Mitra)

Abstract

A Novel type of C-H-σ supramolecular interactions involving σ-aromatic M_2X_2 (M=Cu, Hg; X=Cl, Br, I, S) cores is reported for the first time. Three new polymeric coordination copper complexes, $\{[Cu(\mu\text{-}Cl)(Cl)(\mu\text{-}L)]_2\}_n$ **(1)**, $\{[Cu(\mu\text{-}I)(\mu\text{-}L)]_2\}_n$ **(2)** and $[Cu(Br)_2(\mu\text{-}L)(CH_3CN)_2]_2$ (**3**), have been synthesized with the organic ligand α,ω-bis(benzotriazoloxy)propane system (**L**) and halides as counterions. A very interesting C-H/σ supramolecular interaction has been observed in the solid state structure of compound **2** similar to a C-H···π interaction which has been confirmed by Bader's "atoms-in-molecules" AIM analysis. The Nucleus Independent Chemical Shift (NICs) method was used for evaluating the aromatic character of different cores in this study. The influence of the nature of metal ions, bridging atoms, oxidation states, coordination environments around the metal centers on the strength the aromaticity of M_2X_2 cores were theoretically analyzed and explained. The binding ability of the 1-alkoxy-1,2,3-benzotriazole ring to establish π–π and C-H/π interactions and how its coordination to a Cu(I) and Cu(II) ions affects the strength of the aforementioned interactions have been discussed. The electron deficient triazole ring and its π-acidity increases upon coordination of the Cu ion leading to the formation of a lone pair (lp)–π interaction involving the five-membered ring of the ligand have also been analyzed. We have also analyzed the C–H/σ interactions of previously reported X-ray crystal structures of different coordination polymers based on a binuclear copper (I) complex and 2,3-dimethylpyrazine, dithioethers, benzotriazol-1-yl-based pyridyl units as ligands using I as counter-ion. Complex 1 shows antiferromagnetic behavior with magnetic coupling constants $J = -7.9\ cm^{-1}$. Moreover, photoluminescence and TGA studies were also carried out of the complexes.

Introduction

Noncovalent interactions were first recognized by J. D. van der Waals in the 19th century and helped him to reformulate the equation of state for real gases.[1] In 1940 Linus Pauling and Max Delbruck[2] pointed out that the processes of synthesis and folding of highly complex molecules in the living cell involve, in addition to covalent bond formation, an appreciable number of intermolecular interactions. The noncovalent interactions, or van der Waals (vdW) forces, may be a combination of several interactions such as ion pairing, hydrogen bonding, π-π interactions, cation-π interactions, etc. The non-covalent interactions of biological molecules provide the flexibility and specificity required in most important biological processes related to the regulation of metabolism. They provide a sharp contrast with covalent biochemical compounds which supply the structural firmness and the energy reservoir for living systems. Hydrogen bonding, π-π stacking and cation-π, C-H/π interactions are noncovalent bonding interactions which are well accepted in the field of supramolecular chemistry. Anion-π, lone pair-π interactions have also been recognized from the scientific community for the past seven years.[3] This type of non-covalent bonding is being recognized as a supramolecular interaction by chemists. Noncovalent interactions have always been a challenge for experiment and theory. In recent years the concepts of aromaticity and antiaromaticity have been advanced beyond the framework of organic chemistry. Transition-metal systems, such as the active sites of enzymes or other biomolecules which contain transition-metal atoms and clusters have been studied for interest in understanding the structure and bonding in terms of aromaticity and antiaromaticity. In particular, this topic has been extended into organometallic compounds with cyclic cores of metal atom, polynuclear transition metal compounds, transition-metal clusters, clusters of transition metal suboxides and transition-metal clusters embedded in metallo-organic and

inorganic compounds. It has been shown that main group metal clusters, in which the chemical bonding involves only s-AOs and p-AOs, may possess multiple aromaticity (σ- and π-), multiple antiaromaticity (σ- and π-), and conflicting aromaticity (σ-aromaticity and π-antiaromaticity or *viceversa*). In the transition metal clusters in which d-orbitals are involved in chemical bonding σ-tangential (σ_t-), σ-radial (σ_r-), π-tangential (π_t-), π-radial (π_r-), and δ-aromaticity/antiaromaticity could occur. In this case, there can be triple (σ-, π-, and δ-) aromaticity, triple (σ-, π-, and δ-) antiaromaticity, and a variety of conflicting aromaticities (all combinations of σ-(anti)aromaticity, π-(anti)aromaticity, and δ-(anti)aromaticity). In addition, the number of all-transition-metal aromatic/antiaromatic systems reported in the literature has grown enormously [4-41].

Now the question is whether there is any kind of supramolecular interactions such as cation/σ, C-H/σ, anion/σ, lone-pair/σ similar to cation/π, C-H/π, anion/π, lone pair/π possibly involving σ-aromaticity in transition metal-cluster. What will be the distortion in structural moiety of transition metal cluster while it comes close to proton or lone pair environment? What will be the nature of chemical bonding or aromaticity in transition metal-cluster while it comes close to proton or lone pair environment? Our objective was to synthesize suitable transition metal complex having σ-aromaticity and finding the possibility of supramolecular interaction in the complex and rationalize the interaction using density functional theory (DFT) calculations.

Theoretical methods and Experimental Section

Theory: The energies of all complexes included in this study were computed at the BP86-D3/def2-TZVPD level of theory within the program TURBOMOLE version 6.4.[42] For iodine atom, this basis set uses the ECP28MDF pseudopotential. The interaction energies were calculated with correction for the basis set superposition error (BSSE) by using the Boys-

Bernardi counterpoise technique.[43] For the calculations we have used the BP86 functional with the latest available correction for dispersion (D3). For the calculations involving X-ray structures we have used the crystallographic coordinates. For complexes **16–27** the optimizations have been performed imposing C_{2v} symmetry. Therefore the geometries do not correspond to the global minimum structures. The global minimum is a hydrogen-bonded complex where the halogen atom of the core acts as hydrogen bond acceptor. However, the aim of this manuscript is not to find the most favorable orientation for the complex between acetylene and the M_2X_2 core, instead it is to know if the C–H/σ interaction found in X-ray structures is energetically favorable. The NICS calculation has been performed at the BP86/6-311+G* level of theory using the Gaussian-03 package.[44] For the cores involving iodine, the LANL2DZ basis set has been used for this atom. The "atoms-in-molecules" (AIM)[45] analysis was performed at the BP86/def2-TZVP level of theory. The calculation of AIM properties was done using the AIMAll program.[45b]

Materials: All the chemicals were purchased from sigma Aldrich and used without purification. Solvents were analytical grade.

Synthesis of the ligand [1, 5-bis(benzotriazol-1-yl)-1,5-dioxapentane] (L)

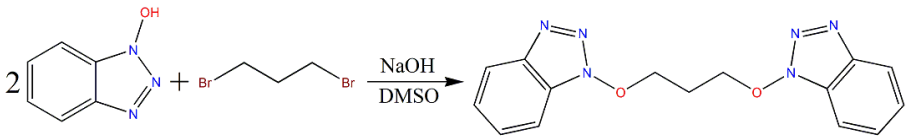

Scheme **I**: Synthetic scheme of the ligand **L**

The ligand (see Scheme **I**) was synthesized by reacting 1-Hydroxybenzotriazole (HOBT) with 1,3-dibromopropane in presence of triethylamine in acetonitrile. HOBT (10 mmol, 1.35 g) was

taken in 20 mL acetonitrile and 1,3-dibromopropane (5 mmol, 1.005g) was added into it. Then triethylamine (10 mmol, 0.505g) was added dropwise and stirred for an half an hour at room temperature. A white solid was precipitated, filtered and washed with acetonitrile. This solid was used for the synthesis of complexes. Yield: 1.272g (80%). Elemental analysis, Found: C, 56.57; H, 4.40; N, 8.76. $C_{15}H_{14}N_6O_2$ requires C, 56.60; H, 4.43; N, 8.8%. FT-IR (KBr, ν_{max}/cm^{-1}): 3060(s), 2957(s), 1466(w), 1447(m), 1399(m), 1366(m), 1345(m), 1265(m), 1241(m), 1160(w), 1108(m), 1090(s), 1030(s), 931(s), 893(w), 777(m), 764(m). UV-vis, $\lambda_{max}(CH_3CN)$/nm: 204, 255 and 283. δ_H NMR (300 MHz, $CDCl_3$, Me_4Si): 2.84 (2H, t, J = 5.11Hz, H^b), 4.9 (2H, t, J = 5.22Hz, H^a), 7.42 (1H, t, J = 7.5Hz, H^d), 7.55 (1H, t, J =7.49Hz, H^e), 7.7(1H, d, J= 8.2Hz, H^f), 8.05(1H, d, J = 8.3Hz, H^c) ppm (Scheme S**1, ESI**). ESI-MS, *m*/*z* (M^+, %):311[M + H^+, 10], 333 [M + Na^+, 100].

Synthesis of complex {[Cu(*μ*-Cl)(Cl)(*μ*-L)]$_2$}$_n$ (1)

$CuCl_2.2H_2O$ (1 mmol, 0.17 g) was dissolved in 20ml acetonitrile solvent. Then an acetonitrile solution (20mL) of the ligand (1mmol, 0.31g) was added dropwise and the mixture stirred for two hour at room temperature, filtered and left for slow evaporation. After one week, rhombohedra shaped yellow crystals were obtained suitable for single crystal x-ray analysis. Yield: 0.25g (70%). Elemental analysis, Found: C, 40.48; H, 3.12; N, 18.85 $C_{15}H_{14}Cl_2CuN_6O_2$ requires C, 40.51; H, 3.17; N, 18.9%. FT-IR (KBr, ν_{max}/cm^{-1}): 3068(w), 2980(w), 1621(w), 1994(w), 1496(w), 1469(w), 1447(m), 1407(m), 1363(m), 1342(m), 1280(m), 1245(m), 1214(m), 1194(w), 1162(m), 1109(m), 1025(m), 952(m), 922(w), 779(w), 766(m),741(s).

Synthesis of $\{[Cu(\mu\text{-}I)(\mu\text{-}L)]_2\}_n$ (2)

CuI (1 mmol, 0.19 g), KI (1mmol, 0.166g) and ligand (1mmol, 0.31g) were taken in 20mL acetonitrile solvent. The mixture was refluxed for 2 hrs. Then it was cooled to room temperature, filtered and left for slow evaporation. After one week, rhombohedra shaped yellow crystals were obtained suitable for single crystal X-ray analysis. Yield: 0.3g (65%). Elemental analysis, Found: C, 35.90; H, 2.80; N, 16.75 $C_{15}H_{14}CuIN_6O_2$ requires C, 35.98; H, 2.82; N, 16.78%. FT-IR (KBr, ν_{max}/cm^{-1}): 3094(w), 2961(w), 1593(w), 1491(w), 1466(m),1443(m), 1364(m), 1343(m), 1269(w), 1238(s), 1217(w), 1173(m), 1152(w), 1124(w), 1103(s), 1083(w), 1030(s), 997(w), 939(m), 920(s), 767(s), 742(s). UV-vis bands, $\lambda_{max}(CH_3CN/nm)$: 378, 346, 328, 313, 234.

Synthesis of $[Cu(Br)_2(\mu\text{-}L)(CH_3CN)_2]_2$ (3)

$CuBr_2$ (1 mmol, 0.223 g) and ligand (1mmol, 0.31g) were dissolved in 20mL acetonitrile. Then the solution was refluxed, cooled to room temperature, filtered and left for slow evaporation. After one week, blocked shaped brown crystals were obtained suitable for single crystal X-ray analysis. Yield: 0.85g (70%). Elemental analysis, Found: C, 35.50; H, 2.95; N, 17.0 $C_{34}H_{34}Br_4Cu_2N_{14}O_4$ requires C, 35.53; H, 2.98; N, 17.06%. FT-IR (KBr, ν_{max}/cm^{-1}): 3473(m), 3067(s), 2977(m), 2919(m), 1611(w), 1495(w), 1467(w), 1447(m), 1420(w), 1406(m), 1363(s), 1342(m),1302(w), 1279(s), 1244(s), 1215(w), 1194(m), 1161(s), 1132(m), 1110(s), 1024(s), 997(w), 952(s), 921(s), 850(w), 779(s), 765(s), 740(s), 641(w), 622(w), 528(m), 429(m).

Physical measurements

The Fourier Transform Infrared spectra (4000-400cm^{-1}) of the ligand and its complexes were recorded on a Perkin-Elmer RX-I FT-IR spectrophotometer in solid KBr matrix. The electronic

spectra of the ligand and complexes were recorded at room temperature on a Perkin-Elmer λ 40 UV/Vis spectrometer in acetonitrile medium. Elemental analyses (C, H, and N) were carried out with a Perkin-Elmer 2400 II elemental analyzer. ^{1}H NMR spectrum of the ligand was recorded on a Bruker 300 MHz FT-NMR spectrometer using trimethylsilane as internal standard in $CDCl_3$. The positive ion ESI-MS for ligand was performed in a QTOF micro mass spectrometer. Variable-temperature magnetic susceptibility measurements were carried out with a Quantum Design MPMS-5S SQUID magnetometer under an applied magnetic field of 5000Oe. Diamagnetic corrections were estimated from Pascal's tables and magnetic data were corrected for diamagnetic contributions of the sample holder. The temperature dependence of the molar magnetic susceptibility, χ_M, was measured on a polycrystalline sample in the temperature range 5 - 300 K. Luminescence spectra were recorded on a Horiba Jobin Yvon Fluorolog 3 spectrometer using a 450 W Xe lamp as excitation source. The spectra were recorded in the solid state in 2 mm inner diameter quartz tube in the reflection mode. Phosphorescence spectra were obtained with a pulsed Xe lamp adapted on the spectrometer. Thermogravimetric analyses were carried out with a heating rate of 10ºC min^{-1} with a Mettler-Toledo Star TGA/SDTA-851 thermal analyser system in a dynamic atmosphere of N_2 (flow rate 80 mL min^{-1}), using alumina crucibles in a temperature range of 25-600ºC

Crystallographic data collection and structure refinements

Good quality single crystals of **1**, **2** and **3** were mounted on a Bruker APEX-II CCD, Philips PW 1100 and Bruker SMART 1000 CCD diffractometer equipped with graphite monochromatized Mo Kα radiation (λ = 0.71073 Å) fine-focus sealed tubes respectively. For **1** and **3**, intensity data were collected at 294(2) using ω scans while for 2 the $\omega/2\theta$ scan technique was used. Crystal

data were collected using the Bruker APEX-II and SMART programs for **1** and **3** respectively, while the FEBO[46a] system was used for **2**. Data refinement and reduction were performed using the Bruker SAINT[46b] software for **1** and **2** and the FEBO system for complex **3**.

Multi-scan absorption corrections were applied to the intensities of **1** and **2** (*T*min = 0.780 and *T*max = 0.923 for **1**, *T*min = 0.330 and *T*max = 0.772 for **3)** using SADABS[46b] while a psi-scan correction[46c] was applied to the intensity data of **2** (*T*min= 0.532 and *T*max= 0.651). The structures were solved by direct methods using the program SIR97,[46d] and refined with full-matrix least-squares based on F^2 using program SHELXL-97.[46e] All non-hydrogen atoms were refined anisotropically. C-bound hydrogen atoms were placed geometrically and refined using a riding model approximation. The molecular graphics and crystallographic illustrations for **1, 2** and **3** were prepared using Bruker SHELXTL[46f] and ORTEP[46g] programs. All relevant crystallographic data and structure refinement parameters for **1**, **2** and **3** are summarized in Table **3**. Selected bond lengths and angles for complexes **1**, **2** and **3** are compared in Table **1**.

Table **1:** Crystal Structure Parameters for **1**, **2** and **3**

	1	**2**	**3**
Empirical formula	$C_{15}H_{14}Cl_2CuN_6O_2$	$C_{15}H_{14}ICuN_6O_2$	$C_{34}H_{34}Br_4Cu_2N_{14}O_4$
Formula weight (g mol^{-1})	444.76	500.76	1149.47
Temperature/K	294K	294K	294 K
Crystal system	Triclinic	Triclinic	Monoclinic
Space group	*P*-1^{-}	*P*-1	*C2/c*
a /Å	9.5074(5)	9.7653(8)	8.9859(11)
b /Å	9.5783(5)	10.1887(11)	17.166(2)
c /Å	11.9155(6)	10.3492(12)	27.480(3)
α /°	96.8542(7)	101.924(3)	90
β /°	105.6088(7)	97.576(2)	90.734(2)
γ /°	117.5410(6)	115.951(3)	90
V/Å^3	888.09(8)	876.51(16)	4238.5(9)
Z	2	2	4
d_{calc} /g cm^{-3}	1.663	1.897	1.801
μ /mm^{-1})	1.554	3.029	4.830
F(000)	450	488	2264
θ range /º	1.9-25.3	3.13-25.5	1.5-25.5
measured reflections	9893	3459	21533
independent reflections	3222	3258	3971
R_{int}	0.019	0.019	0.070
goodness-of-fit on F^2	1.09	1.012	1.01
Observed data	2891	2554	2602
final *R* indices [$I > 2\sigma(I)$]	*R*1=0.0323	*R*1 = 0.0461	*R*1=0.0519
	$wR^2 = 0.0992$	$wR^2 = 0.1298$	$wR^2 = 0.1294$
R indices (all data)	*R*1=0.0366	*R*1 = 0.0608	*R*1 = 0.0885
	$wR^2 = 0.0962$	$wR^2 = 0.1229$	$wR^2 = 0.1199$
$\Delta\rho_{min}$/e Å^{-3} and $\Delta\rho_{max}$/e Å^{-3}	-0.41, 0.96	-1.10, 1.13	-0.78, 0.80

Result and discussion

Description of crystal structure

{[Cu(μ-Cl)(Cl)(μ-L)]$_2$}$_n$ (1): The X-ray single-crystal diffraction analysis reveals that complex **1** crystallizes in *P-1*space group of the triclinic crystal system. The asymmetric unit of **1** (**Fig. 1**) contains one neutral ligand **L**, one copper (II) atom and two chloride ions. In **1** the coordination polyhedron around the copper(II) centre could be described as distorted square pyramidal (τ = 0.22)[47] with atoms Cl1, N1, Cl2, and Cl2^{i} [symmetry code: (i) 1-x,-y,-z] forming a remarkably

tetrahedrally distorted basal plane (maximum displacement 0.333(3) Å for atom N1) and atom $N6^{ii}$ [symmetry code: (ii) 2-x, 1-y,1-z] at the apex, with the metal displaced by 0.2549(4) Å toward N6 from the mean basal plane. The relative deviations of bond angles and lengths from the ideal values (Table **2**) also support the distorted geometry of the copper(II) centre. The Cu–N and Cu–Cl bond lengths are of 2.019(2)-2.240(2) and 2.2738(7)-2.3395(8) Å, respectively. In **1** two neighbouring units connect each other through double μ-halide bridges, leading to centrosymmetric Cu(μ-Cl)$_2$Cu building blocks (**Fig. 1**). The ligand **L** bridges adjacent Cu(μ-Cl)$_2$Cu units by coordinating the metal centres through the N1 and N6 nitrogen atoms of the benzotriazole units. Thus two well separated Cu(μ-X)$_2$Cu dimeric units in **1** are connected by two long spacer organic ligands resulting in a one-dimensional helical-like metal-organic hybrid architecture extending along the crystallographic [111] direction (**Fig. 2**). The Cu···Cu separation in the Cu(μ-Cl)$_2$Cu units in **1** is 3.4078(6) Å, while the separation between copper(II) metals bridged by the organic spacer is 9.9017(5). The Cu–Cl–Cu bridging angle is 93.91(3)º. In this conformation, no intramolecular hydrogen bond is observed, whereas π–π stacking interactions occur involving the aromatic rings of adjacent benzotriazole units [$Cg1...Cg1^{iii}$ = 3.817(2) Å, perpendicular interplanar distance = 3.3832(16) Å, offset = 1.766(5) Å [*Cg1* is the centroid of the C10–C15 ring; symmetry code: (iii) 2-x, 1-y, 1-z]. In addition, C-H–π interactions [H6...$Cg1^{iv}$ = 2.88 Å, C6... $Cg1^{iv}$ = 3.552(5) Å, C6-H6... $Cg1^{iv}$ = 130°; symmetry code: (iv) 1-x, 1-y, 1-z] connect the chains generating a 2-D extended supramolecular network of the type C-H–π/π–π/π–H-C, as will be further discussed below.

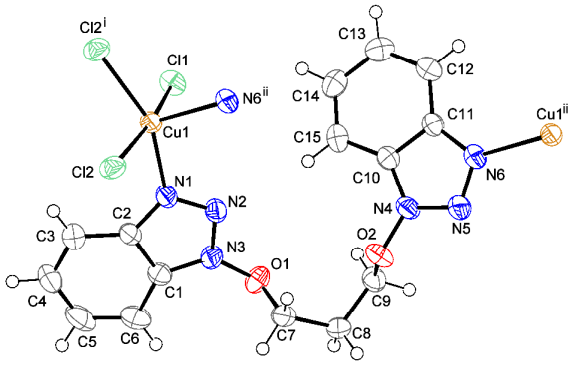

Fig. 1 The asymmetric unit of complex **1** showing displacement ellipsoids drawn at the 50% probability level. Symmetry codes: (i) 1-x, -y, -z; (ii) 2-x, 1-y, 1-z.

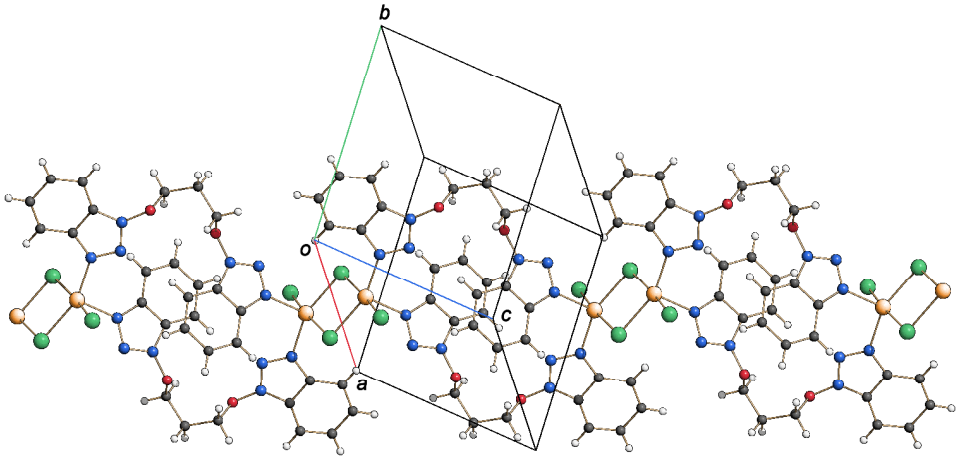

Fig. 2 Partial packing diagram of complex **1** showing a polymeric chain extending parallel to the [111] direction.

{[Cu(μ-I)(μ-L)]$_2$}$_n$ (2): In order to evaluate the influence of the counter-anions with different coordination abilities on the structure of the complex, CuI was used to react with **L** under the same conditions as **1**, and complex **2** was successfully isolated. Compound **2** also crystallizes in the triclinic space group *P-1*. The asymmetric units of **2** contain one neutral ligand **L**, one copper (I) atom and one iodide ion (**Fig. 3**). In **2** the coordination polyhedron around the copper(I) centre could be described as distorted tetrahedral, with atoms I1, N1, I1^{i}, and N6^{ii} with quadratic

elongation 1.033 [symmetry codes: (i) 1-x, -y, 1-z; (ii) 2-x, 1-y, 2-z]. The Cu–N and Cu–I bond lengths are of 2.069(4)-2.075(5) Å and 2.6471(9)-2.6539(9) Å, respectively. As observed in **1**, two neighbouring units connect each other through double μ-halide bridges, leading to centrosymmetric Cu(μ-I)$_2$Cu building blocks (**Fig. 3**). The ligand **L** bridges adjacent Cu(μ-I)$_2$Cu units by coordinating the metal centres through the N1 and N6 nitrogen atoms of the benzotriazole units. Thus two well separated Cu(μ-I)$_2$Cu dimeric units are connected by two long spacer organic ligands to form helical-like chains running parallel to the [111] direction (**Fig. 4**). The Cu...Cu separation in the Cu(μ-I)$_2$Cu units is 2.8439(14) Å, while the separation between copper(I) metals bridged by the organic spacer ligand **L** is 9.5412(11) Å. The Cu–I–Cu bridging angle is 64.89(2)º. Intraligand and intrachain hydrogen interactions are observed [H5···N5 = 2.59 Å, C5···N5 = 3.404(8) Å, C5-H5···N5 = 146°; H14···N2 = 2.60 Å, C14···N2 = 3.458(8) Å, C14-H14···N2 = 154°] and π–π stacking interactions occur within the Cu(μ-I)$_2$Cu building block involving the aromatic rings of adjacent benzotriazole units [*Cg1*···*Cg2*^{i} = 3.629(4)Å, perpendicular interplanar distance = 3.308(3)(16) Å, offset = 1.493(9) Å; *Cg1* is the centroid of the C10–C15 ring; symmetry code: (i) 2-x, 1-y, 1-z]. Similarly to **1**, in the crystal the chains are linked into a 2-D extended supramolecular network of the type C-H–π/π–π/π–H-C by C-H–π interactions [H2···*Cg1*^{ii} = 2.71 Å, C2···*Cg1*^{ii} = 3.287(8) Å, C2-H2···*Cg1*^{ii} = 121°].

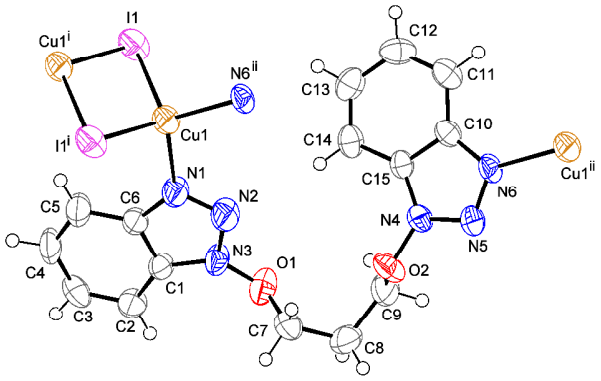

Fig. 3 The asymmetric unit of complex **2** with displacement ellipsoids drawn at the 50% probability level. Symmetry codes: (i) 1-x, -y, 1-z; (ii) 2-x, 1-y, 2-z.

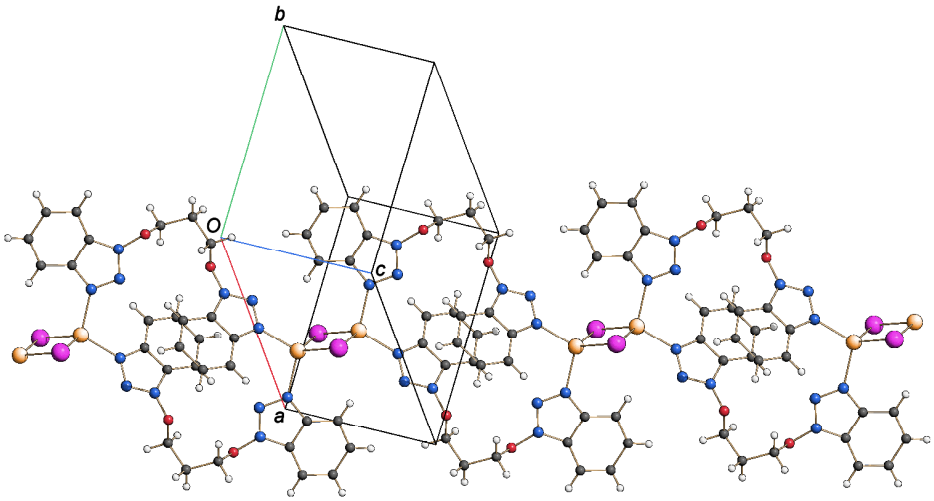

Fig. 4 Partial packing diagram of complex **2** showing a polymeric chain extending parallel to the [111] direction.

$[Cu(Br)_2(\mu\text{-}L)(CH_3CN)_2]_2$ (**3**): The asymmetric units of **3** contains one neutral ligand **L**, one copper (II) atom, two bromide ions and one acetonitrile molecule (**Fig. 5**). In **3** the coordination polyhedron around the copper(II) centre could be described as distorted trigonal bipyramidal, (τ=0.6)[47] with atoms Br1, N4, Br2, forming a the equatorial plane and atoms N1A and N1B at the apices. The copper metal protrudes from the equatorial plane by only 0.0082(5) Å toward atom N1B. The relative deviations of bond angles and lengths from the ideal values (Table **2**) support

the distorted geometry of the copper(II) centre. The Cu–N and Cu–Br bond lengths are in the range 2.000(4)-2.206(5) and 2.4152(9)-2.4689(10) Å, respectively. The ligand **L** bridges adjacent $CuBr_2.CH_3CN$ units by coordinating the metal centres through the N1A and N1B nitrogen atoms of the benzotriazole units. The separation between copper(II) metals bridged by the organic spacer is 7.4132(11) Å. Intramolecular C–H···N hydrogen bonds are observed [H10A···N2B^{i} = 2.62 Å, C10···N2B^{i} = 3.559(9) Å, C10-H10A···N2B^{i} = 167°. Symmetry code: (i) -x, y, 1/2-z]. In the crystal, the complex molecules are connected by intermolecular C–H…Br and C–H···O hydrogen bonds into layers parallel to the *ab* plane [H7B1···O1A^{ii} = 2.52 Å, C7B···O1A^{ii} = 3.438(6) Å, C7B-H7B1···O1A^{ii} = 158°; H10C···Br2^{iii} = 2.71 Å, C10···Br2^{iii} = 3.614(8) Å, C10-H10C···Br2^{iii} = 157°. Symmetry codes: (ii) 1/2-x, -1/2+y, 1/2-z; (iii) 1-x, y, 1/2-z]. The layers are further linked into a 3-D supramolecular network (**Fig. 6**) by C–H…Br hydrogen interactions [H4B... Br1^{iv} = 2.89 Å, C4B…Br1^{iv} = 3.697(6) Å, C4B-H4B…Br1^{iv} = 146°. Symmetry code: (iv) 1/2-x, 1/2-y, -z].

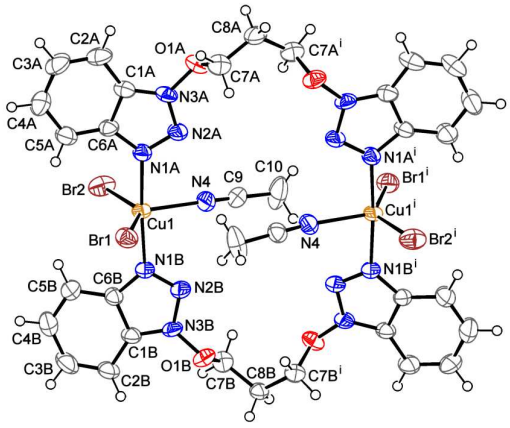

Fig. 5 The molecular structure of complex **3**, showing displacement ellipsoids drawn at the 50% probability level. Symmetry code: (i) -x, y, 1/2-z.

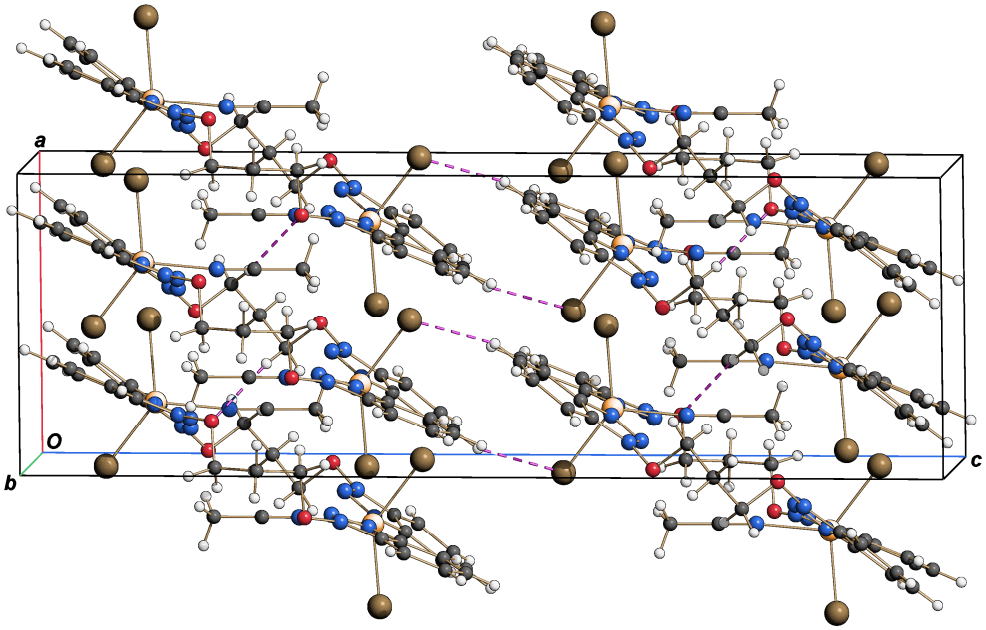

Fig.6 Crystal packing of complex **3** approximately viewed along the *b* axis. Intermolecular hydrogen bonds are shown as dashed lines.

Table **2**: Selected bond lengths and bond angles for **1**, **2** and **3**

1		**2**		**3**	
Cu1-Cl1	2.2738(7)	Cu1-I1	2.6471(9)	Cu1-Br1	2.4152(9)
Cu1-Cl2	2.3395(8)	Cu1 -I1^{iii}	2.6539(9)	Cu1-Br2	2.4689(10)
Cu1-Cl2^{i}	2.3236(8)	Cu1-N1	2.075(5)	Cu1-N1A	2.000(4)
Cu1-N1	2.019(2)	Cu1-N6^{iv}	2.069(4)	Cu1-N1B	2.011(4)
Cu1-N6	2.240(2)			Cu1-N4	2.206(5)
Cl1-Cu1-Cl2	168.95(3)	Cu1-I1-Cu1^{iii}	64.89(3)	Br1-Cu1-Br2	137.91(4)
Cu1-Cl2-Cu1^{i}	93.91(3)	I1-Cu1-N1	102.09(15)	Br1-Cu1-N1A	89.86(13)
Cl1-Cu1-N1	90.18(8)	I1-Cu1-I1^{iii}	115.11(3)	Br1-Cu1-N1B	89.14(13)
Cl1-Cu1-Cl2^{i}	91.55(3)	I1-Cu1-N6^{iv}	111.55(12)	Br1-Cu1-N4	122.30(15)
Cl1-Cu1-N6^{ii}	97.43(7)	N1 -Cu1-N6^{iv}	109.61(18)	Br2 -Cu1-N1A	90.20(14)
Cl2-Cu1-N1	87.56(8)	I1^{iii}-Cu1-N6^{iv}	109.89(12)	Br2-Cu1-N1B	93.30(13)
Cl2-Cu1-Cl2^{i}	86.09(3)			Br2-Cu1-N4	99.79(15)
Cl2-Cu1-N6^{ii}	93.61(7)			N1A-Cu1-N1B	175.77(19)
Cl2^{i}-Cu1-N1	155.52(8)			N1A-Cu1-N4	89.21(18)
N1-Cu1-N6^{ii}	104.18(1)			N1A-Cu1-N4	87.86(18)
Cl2^{i}-Cu1-N6^{ii}	99.80(7)				

Symmetry codes: (i) 1-x,-y,-z; (ii) 2-x, 1-y, 1-z; (iii) 1-x, -y, 1-z; (iv) 2-x, 1-y, 2-z.

Magnetic study

The temperature dependence of the molar magnetic susceptibility for complex **1**, χ_M, was measured on a polycrystalline sample in the temperature range 5 - 300 K. The experimental points are drawn in black squares and the calculated curves are in red line (**Fig. 7**) The $\chi_M T$ value at room temperature is about 0.76 cm^3 K mol^{-1}, in good agreement with two uncoupled spins 1/2 with a Landé factor g=2.05. The $\chi_M T$ values remain constant down to about 60 K. When the temperature is decreased below 60 K, a decrease in $\chi_M T$ is observed, to reach the value of 0.37 cm^3 K mol^{-1} at 5 K.

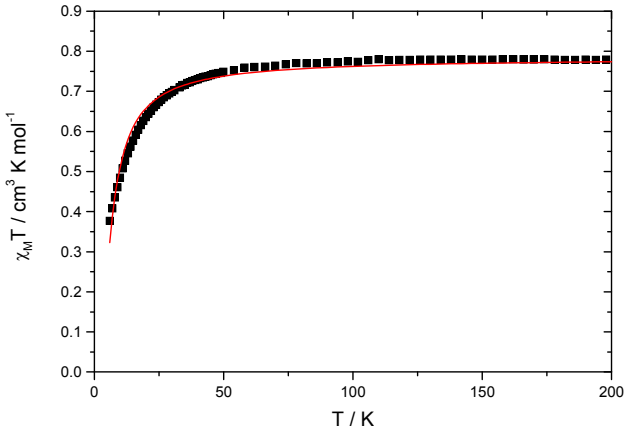

Fig. 7 Thermal variation of the $\chi_M T$ product per Cu(II) dimer for compound **1**.

It is found that the upper atoms form a chain and two coppers atoms are alternatively bridged by two organic ligands and two chlorine atoms. Due to the large size of the ligand, it can be safely assumed that no magnetic interaction can take place through the organic bridge. From a magnetic point of view, the compound can be considered as copper dimers linked by two chlorido bridges. In line with the dimeric nature of the compound, the magnetism has been fitted using a classical Bleanay and Bowers law:

$$\chi_M T = \frac{N\beta^2}{3k_B}\frac{2g^2}{1+\exp\left(-J/k_B T\right)/3}$$

Best fit was obtained with g = 2.05 and J = -7.9 cm^{-1}. The magnetic interaction in halo-bridged dinuclear compounds has been extensively studied, experimentally and theoretically. A complete DFT study has been undertaken by Ruiz *et al*.[48] In this article, they emphasize that three different geometries of dinuclear dihalo-bridged Cu(II) complexes with square pyramidal environment have been experimentally characterized: square pyramids sharing a basal edge (**I**), square pyramids sharing a base-to-apex edge with parallel basal planes (**II**), and square pyramids that also share a base-to-apex edge, but with perpendicular basal planes (**III**) (Scheme **II**).

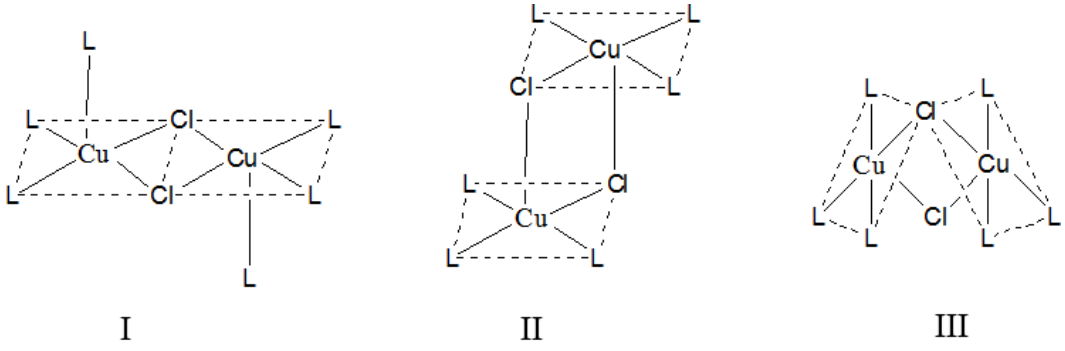

Scheme **II.** Three different geometries of dinuclear dihalo-bridged Cu(II) complexes

Complex **1** clearly belongs to the type **I** geometry where the pyramids share a basal edge (I). Several compounds have been described where the terminal is a Cl ion[49] as well as a few compounds where the two terminal atoms are N atoms.[50a] In particular; it has been observed that the interaction is ferromagnetic in the case of N-donor terminal ligands L, whereas it is antiferromagnetic for halide ions as terminal ligands. Theoretical prediction done by DFT has shown that the J values should be negative when the angle Cu-Cl-Cu is larger than 98° and

positive below this value for a model compound $[Cu_2Cl_2(NH_3)_6]$ with Cu-Cl distance of 2.31 Å. Having an angle Cu-Cl-Cu of 93.91°, complex **1** should present a ferromagnetic interaction of about +40 cm^{-1}. However, when the terminal ligands NH_3 are replaced by Cl atoms, DFT calculations predict a *J* coupling constant between -30 and -59 cm^{-1}. Thus, theoretical calculations confirm the experimental observation, that is to say, the ferromagnetic character of the interaction for N terminal ligand and the antiferromagnetic interaction for Cl terminal ligand. Complex **1** presents both Cl and N terminal ligands. Thus, it can be expected that *J* coupling constant will be intermediate between the case of complexes with N terminal or Cl terminal only ligands. With a moderate antiferromagnetic *J* coupling of -7.9 cm^{-1}, it is indeed the case. Finaly, a compound having type I geometry and both Cl and N terminally coordinated ligands has been described, having a small antiferromagnetic *J* coupling constant of -3.72 cm^{-1}.[50b] This value is in line with the small antiferromagnetic value obtained for complex **1**.

Photophysical study

The photo-physical study of the complexes was performed at 298 K in the solid state. The excitation and emission spectra of the compound are presented in the **Fig. 8**. Upon excitation in the UV domain (360 nm), the emission spectrum displayed a weak emission signal with two distinct maxima at 415 and 435 nm with a shoulder around 480 nm. Whatever the selected emission wavelength (415, 435 or 480 nm), the corresponding excitation spectra displayed a broad and structured excitation band with a maximum at 365 nm and shoulders on the high and low energy tails (respectively at 340 and 401 nm). Attempts to gain insights into the luminescence lifetime of the emitted signal were unsuccessful with our experimental set up, indicating a lifetime shorter than *ca* 20 μs.

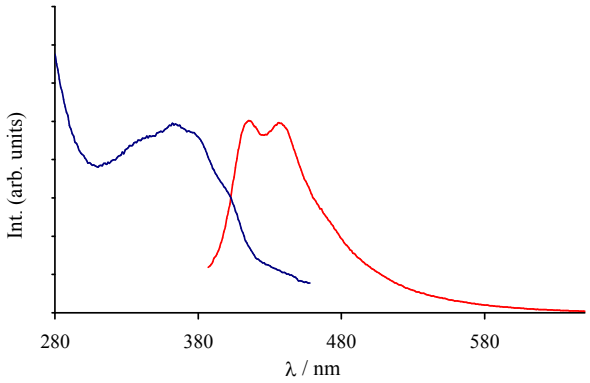

Fig. 8 Excitation (blue, λ_{em} = 480 nm) and emission (λ_{exc} = 360 nm) spectra of $[Cu_2(\mu_2\text{-}I)_2L_4]$ in the solid state at 298K.

Although the luminescence properties of the $[Cu_2(\mu_2\text{-}I)_2]$ systems have been far less studied than the parent $[Cu_4(\mu_3\text{-}I)_4]$ compounds,[51-53] some examples can be found in the literature.[54,55] In concordance to numerous computational studies on these systems[56] their emission spectra are generally composed of a highly low energy emission band originating from a cluster centred triplet excited state (^{3}CC) and a high energy component attributed to a halide to metal triplet excited state (^{3}XMCT). Regarding the rather weak intensity of the emission signal, its energy level and considering the rather long Cu-Cu distance of 2.844 Å, the structured emission band observed in our case may be attributed to a ^{3}XMCT transition. Interestingly, the observed emission spectrum is very similar to that measured for a metallopolymer consisting of distinct rhombic $[Cu_2(\mu_2\text{-}I)_2]$ units linked by diphosphine units,[54] for which the Cu-Cu distance (2.806 Å) is very close to the one observed in our case. These results point to a weak influence of the ancillary ligands (phosphine[54] or benzotriazol in the present case) and the attribution of the emission has originating from the XMCT triplet state.

Theoretical DFT study

As explained above, three new polymeric coordination complexes have been synthesized and X-ray characterized. They are copper complexes where the organic ligand is a *α,ω*-bis(benzotriazoloxy)propane system and also present halides in the solid state acting as counterions (see **Fig. 1** and **3**) and all compounds are polymeric in the solid state. Compound **1** is characterized by having Cu(II) as metal center and chloride as counterion, whereas compound **2** has Cu(I) as metal center and iodide as counterion. In the solid state they present interesting noncovalent interactions that govern the crystal packing, where the π-system plays a prominent role. In the first part of this computational study we have analyzed the binding ability of the 1-alkoxy-1,2,3-benzotriazole ring to establish π–π and C-H/π interactions and how its coordination to a Cu(I) and Cu(II) ions affects the strength of aforementioned interactions.

To perform the computational study we have used the 1-hydroxy-1,2,3-benzotriazole (**HBT**) ring as a model of the ligand. This is an interesting ring, since it combines an electron rich six-membered ring with an electron deficient five membered ring, that certainly condition its π-binding properties. To confirm this issue, we have obtained the molecular electrostatic potential surface (MEPS) of the ring. It can be observed in **Fig. 9** that the electrostatic potential is negative over the six membered ring (6R) and positive over the five-membered ring (5R). Therefore the π–π complex of a dimer of **HBT** should be favored in an antiparallel disposition, since the interaction of the electron-rich ring (6R) with the electron poor (5R) is maximal. We have optimized the π–π complex of this compound at the BP86-D3/def2-TZVPD level of theory, and the final geometry presents an antiparallel displaced arrangement, see **Fig.10**. Interestingly this arrangement is almost identical to that observed experimentally. We have also studied the influence of the coordination to Cu(I) and Cu(II) to the HBT ligand on the stacking energy. In

the theoretical models we have used chloride as counterion in order to keep the model neutral. The stacking is considerably reinforced by the presence of the Cu coordinated to N3, as indicated in **Fig. 10**. In the case of Cu(I) the interaction energy is slightly more favorable than for Cu(II) and the π–π distance is shorter, in agreement with the experimental results.

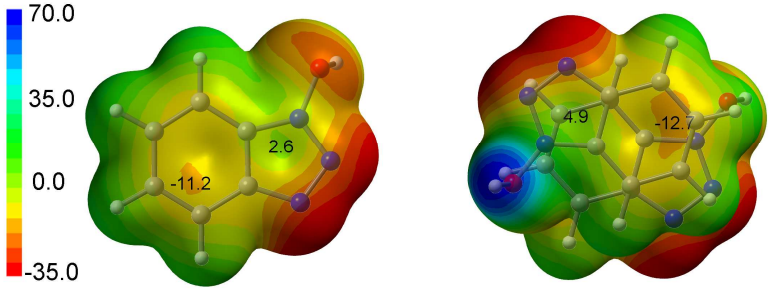

Fig. 9 MEPS of the **HBT** (left) and the π–π stacked dimer of **HBT** (right). The value of MEP iver the six and five membered rings are also indicated in kcal/mol.

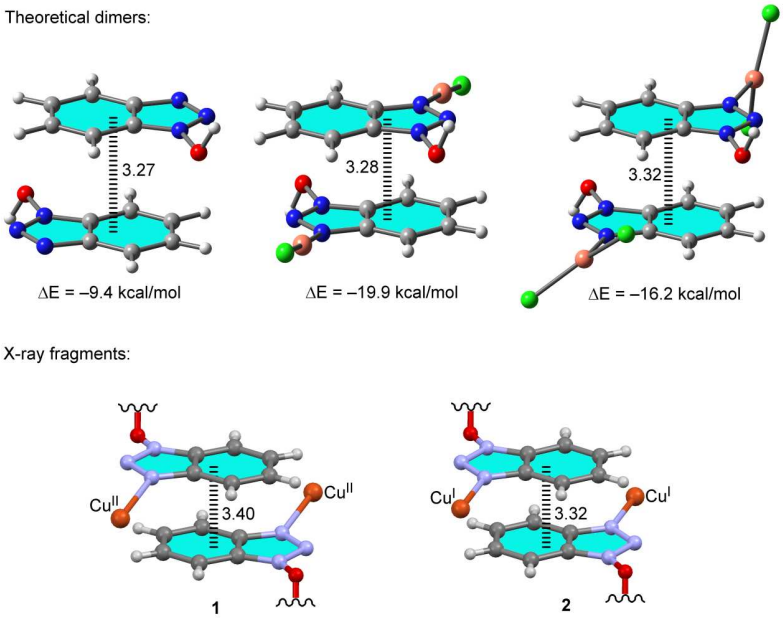

Fig. 10 Top: Interaction energies of the optimized dimers are shown (distances in Å). 1-hydroxy-1,2,3-benzotriazole (**HBT**) ring is used as a model of the ligand. Bottom: X-ray fragments of compounds **1** and **2**, where similar synthons are observed.

We have also studied the ability of the ligand to establish C-H/π interactions, since they are observed in the solid state structures. In addition, we have studied the influence of the stacking interaction on the C-H/π interaction. We have used methane as C-H donor and the energetic results are shown in **Fig. 11**. The interaction energy of a single molecule of **HBT** and methane is –2.1 kcal/mol and the interaction with the stacked dimer of **HBT** is slightly more favorable, indicating that there are not relevant cooperativity effects between both interactions. This C-H/π–π assembly is observed in the crystal structure of both compounds. The agreement between the computed and experimental C-H/π distances is remarkably, specially for the Cu(I) structure (see **Fig. 11**). We have also analyzed computationally the effect of the copper atom on the C-H/π interaction. We have not observed a significant influence of the coordination of either Cu(II) or Cu(I) on the energetic features of the interaction, probably due to the fact that the coordination is produced on the triazole ring and the C-H/π interaction involves the phenyl ring

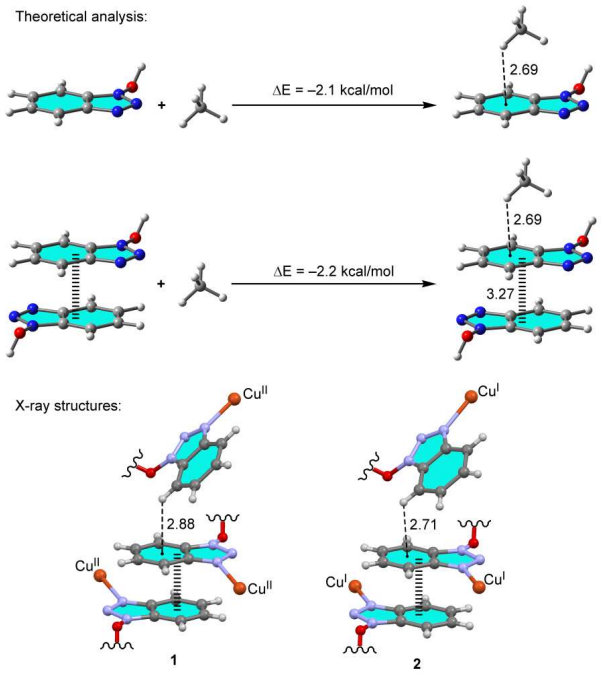

Fig. 11 Top: Binding energies for the C-H/π interactions are shown (distances in Å). 1-hydroxy-1,2,3-benzotriazole (**HBT**) ring is used as a model of the ligand. Bottom: X-ray fragments of compounds **1** and **2**, where similar arrangements are observed.

A very interesting interaction has been observed in the solid state structure of compound **2** that deserves an especial attention. It is similar to a C-H/π interaction; however a sigma system participates in the interaction instead of a π-system. Recently, it has been demonstrated that dinuclear Cu(II) complexes with rhombus [Cu_2X_2] cores exhibit σ-aromaticity that unprecedentedly interact with two closely disposed coordinated perchlorate ions, establishing anion–σ interactions.[57a] A close examination of the solid state structure of **2** reveals that the Cu_2I_2 core is close to an aromatic C-H bond. In order to study the importance of this interaction we have first optimized a complex between a model of this core and HC≡CH as hydrogen bond donor. It should be mentioned that the acidity of the hydrogen atom acetylene is higher than the aromatic hydrogen atom that participates in the interaction in complex **2**. However, we have selected this linear model molecule to avoid other secondary interactions with the ligands of the Cu atoms and to characterize and analyze the interaction in general using a theoretical model. The energetic analysis in a more elaborated model of compound **2** is further described below. The complex (named C-H/σ) presents favorable interaction energy (–9.6 kcal/mol, see **Fig. 12**), which confirms the relevance and strength of this new interaction. We have also computed the interaction energy of this complex where the HCCH molecule has been fixed at 2.94 Å from the ring centroid, which is the distance of the C-H/σ interaction in the crystal structure. The binding energy is only reduced to –6.8 kcal/mol, indicating that the interaction is nevertheless important at this longer distance. We have performed the Bader's "atoms-in-molecules" AIM analysis of this complex in order to characterize the interaction since it provides an unambiguous definition

of chemical bonding.[44] As a matter of fact, the bond path has been used to characterize a number of noncovalent interactions of several sorts. It can be observed that the C-H/σ interaction is characterized by the presence of two bond critical points (red spheres in **Fig. 12**) that connect the hydrogen atom with the metal centers (dashed bond paths). The Laplacian of the electron density at the bond critical points that characterize the interaction is 2.3×10^{-2} a.u. A positive value of the Laplacian at the bond critical point is common in non covalent interactions. Moreover, we have also computed the ellipticity at the bond critical points that provides a measure of the anisotropy of the curvature of the electron density in the directions normal to the bond (a zero value indicating no anisotropy). Therefore it serves as a sensitive index to monitor the π character of bonds. The ellipticity is ε = 4.83 a.u. that is indicative of a certain anisotropy in this interaction likely due to the participation of the Cu orbitals. In **Fig. 12**, we also show the X-ray structure of compound **2** where the double C-H/σ interaction is highlighted. It can be clearly appreciated the short contacts between the aromatic hydrogen atoms of the ligand and the Cu_2I_2 core. In an effort to estimate the C-H/σ interaction in the X-ray structure we have used the ligand inter-exchange equations shown at the bottom of **Fig. 12**). That is, using the first (top) reaction, we have evaluated the reaction energy upon changing one benzotriazoloxy (BTZ) by a triazoloxy (TAZ) ligand, denoted as ΔE. This energy is associated to one of the C–H/σ interactions. Using the second equation we measure the energy variation of changing both ligands that participate in the interaction (ΔE'). This allows us to evaluate the interaction and possible cooperativity effects by comparison to ΔE. The variation energy for the first equation (ΔE) is 3.9 kcal/mol, indicating that the complex with BTZ ligand is more favorable than the one with TAZ, where the interaction is not formed. The computed value for ΔE' where two simultaneous C–H/σ interactions are evaluated is 7.7 kcal/mol. This value is approximately twice the ΔE energy,

indicating that the interaction is additive in compound **2** and, consequently, cooperativity effects are not present. The interaction energy is smaller than the one estimated for the model system due to two factors. The acidity of the hydrogen atom of the interacting molecule (HCCH) is higher in the model system and the directionality of the interaction in the model system is better than in the crystal structure.

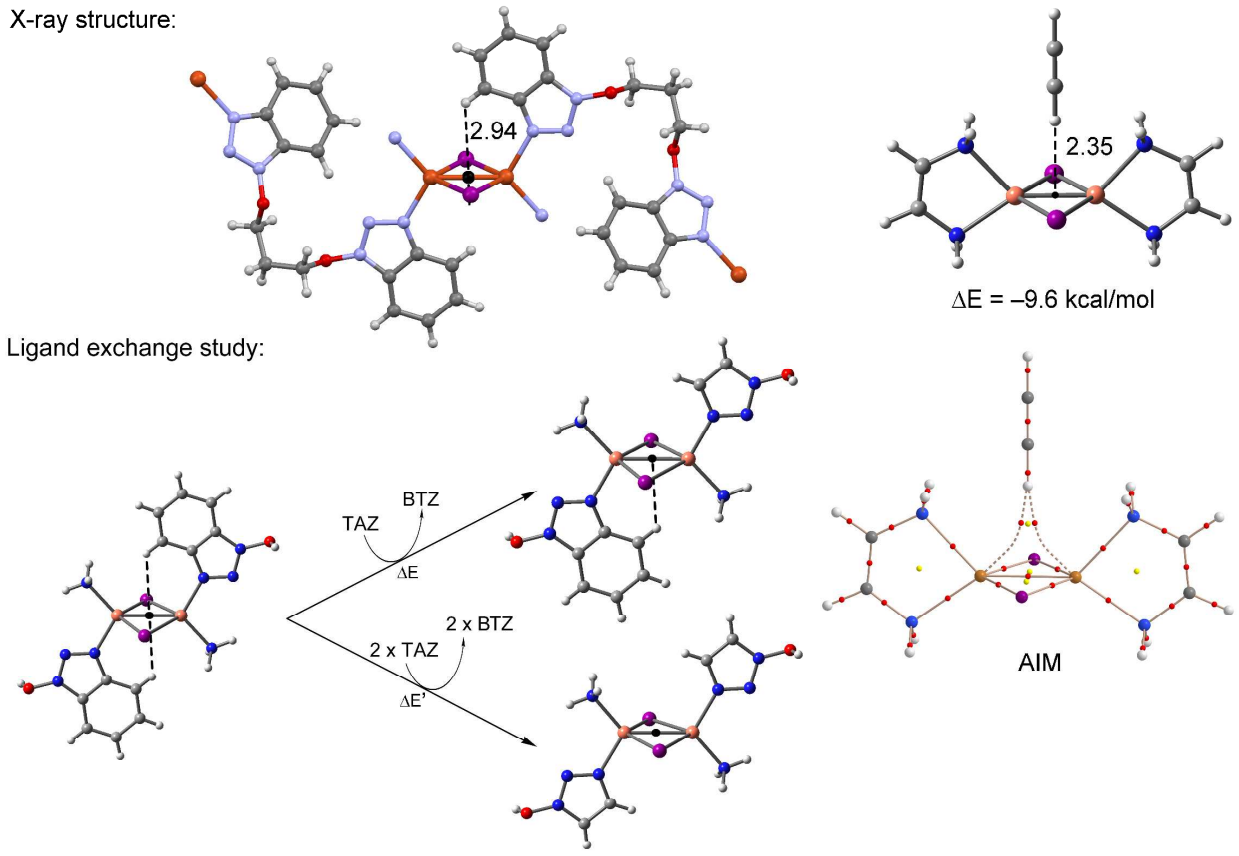

Fig. 12 Top: X-ray fragment of compound **2**, where a double C-H/σ interaction is formed. Top Right: C_{2v}-optimized complex of a theoretical model with the Cu_2I_2 rhombus core interacting with HCCH. Right: AIM analysis of the complex with indication of the bond (red) and ring (yellow) critical points. The bond paths connecting bond critical points are also represented. Bottom: Equations used to compute ΔE and ΔE' energies to estimate the C–H/σ interaction in **2**.

Finally, we have computed the AIM analysis of a large fragment of the crystal structure using the crystallographic coordinates and replacing some ligands by ammonia and the propane chain by a hydrogen atom in order to confirm the existence of the relevant and unprecedented C-H/σ interaction in the solid state of compound **2**. It can be observed in **Fig. 13** that there is a critical point and the corresponding bond path connecting the aromatic hydrogen atom with one copper atom that belongs to the Cu_2I_2 core. The second copper atom of the core participates in the other C-H/σ interaction at the opposite face of the Cu_2I_2 core. In this case, only one bond critical point characterizes each interaction in contrast to the behavior observed in the theoretical model (*vide supra*). The Laplacian of the charge density at the bond critical point is positive (1.15×10^{-2} a.u.) as is common in interactions between closed-shell systems and the ellipticity is ε = 0.81 a.u. indicating that the anisotropy of the bond is significantly reduced with respect to the theoretical model. This is likely due to the directionality of the C-H bond that is conditioned by the intramolecular nature of the interaction. In addition, this distribution of critical points may indicate the possibility to consider it as an agostic interaction[57b], which is common between coordinatively-unsaturated transition metal and the two electrons involved in the C-H bond. However the Cu···H–C angle observed in compound **2** is likely too large (153.4º) for considering it as an agostic interaction that is characterized by angles ranging 90–140°.

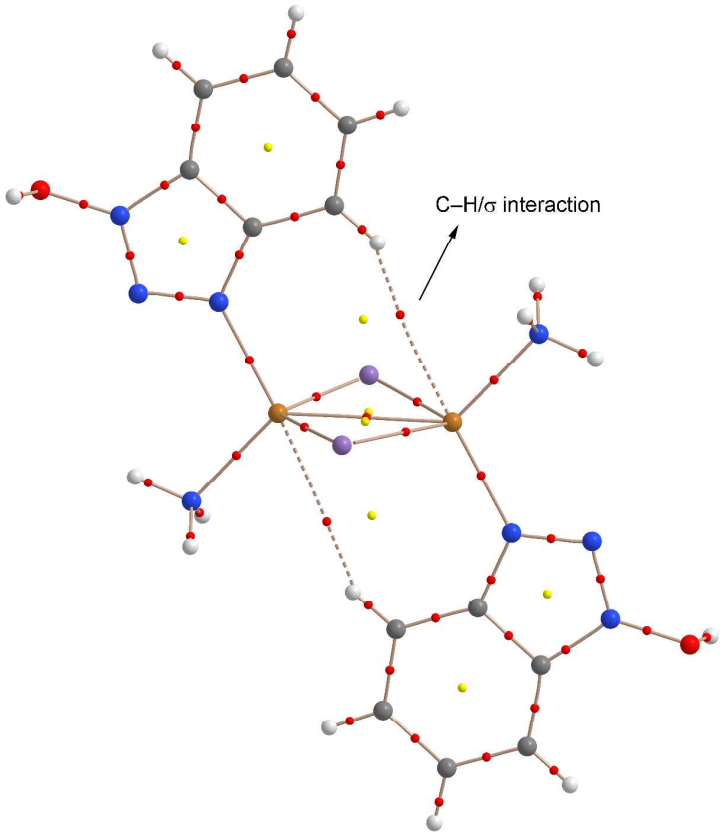

Fig. 13 AIM analysis of a crystal fragment where two ligands are replaced by ammonia and the alkyl chain by a hydrogen atom. Bond and ring critical points are represented by red and yellow spheres, respectively.

Apart from the polymeric compounds **1** and **2**, a dimeric structure (**3**) has also been obtained (see **Fig. 5**). It is a copper (II) metallomacrocyclic structure formed by two units of the organic ligand α,ω-bis(benzotriazoloxy)propane system, with bromine atoms acting as counterions. Two solvent molecules of CH_3CN are also coordinated to the copper (II) metal centers. Interestingly, both solvent molecules participate in relevant hydrogen bonding interactions with the bromido ligands in the solid state. In **Fig. 14**, we represent a fragment of the crystal structure highlighting this interaction and a theoretical model used to estimate its energetic value. For the theoretical model we have used 1-hydroxy-1,2,3-benzotriazole as ligand. The interaction energy of the H-bonded dimer is –10.5 kcal/mol and consequently each hydrogen

bond contributes by –5.25 kcal/mol to the stabilization of the complex. It should be mentioned that the electron density around the bromine atom is not spherical but anisotropically distributed, with a charge concentration in the equatorial area, and charge depletion along the Cu-Br axis, which is named "σ-hole". In this case the Cu–Br···H angle is 140º, which likely suggest that the hydrogen atom is mainly pointing to the belt of the negative electron density around the bromine atom.

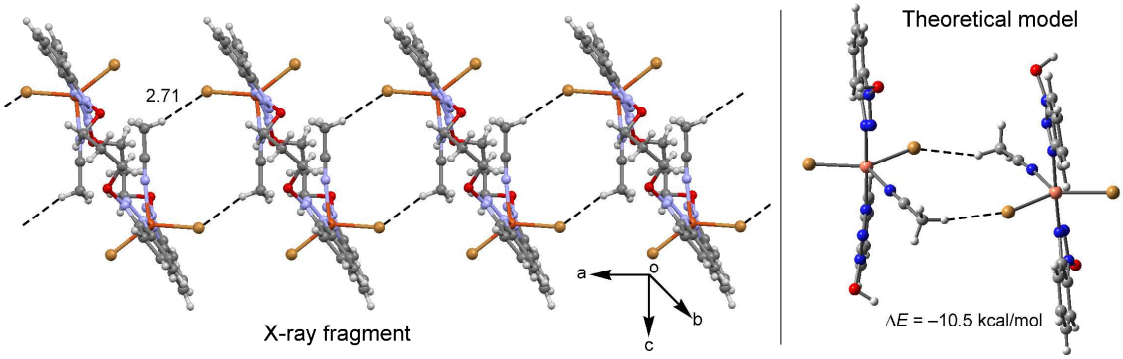

Fig. 14 X-ray fragment showing the intermolecular doubly C–H···Br hydrogen bonds and the theoretical model. Distances in Å.

Finally, we have analyzed the crystal growth in the *b* direction (see **Fig. 15**), where the presence of intermolecular hydrogen bonds results in the formation of layers as explained in the description of the structures. The formation energy of one dimer of this infinite column is –41.2 kcal/mol, where several hydrogen bonds and other conventional interactions are established. Among them, we have focused our attention to the formation of a lone pair (lp)–π interaction involving the five-membered ring of the ligand (see **Fig. 15**, bottom left). As previously described using the MEP surface, the triazole ring is electron deficient and its π-acidity further increases upon coordination of the Cu ion. Therefore it is well-suited for the interaction with lone-pair donor atoms. We have evaluated this interaction using a theoretical model where, apart

from using 1-hydroxy-1, 2, 3-benzotriazole as ligand, one of the ligands has been replaced by an ammonia in order to keep the size of the system computationally approachable. The interaction energy is very favorable (–14.6 kcal/mol). However this energy also includes the contribution of a weak hydrogen bond between the aromatic hydrogen atom of one ligand and the chloride ligand of the other complex. In order to know the contribution of this hydrogen bond, we have computed the binding energy of an additional model where one benzotriazole ligand has been replaced by a triazole. The interaction energy is then reduced to –12.2 kcal/mol indicating that the hydrogen bond contributes only by –2.4 kcal/mol and that the lp–π interaction is certainly important in the stabilization of this complex and, consequently, in the solid state architecture of compound **3**.

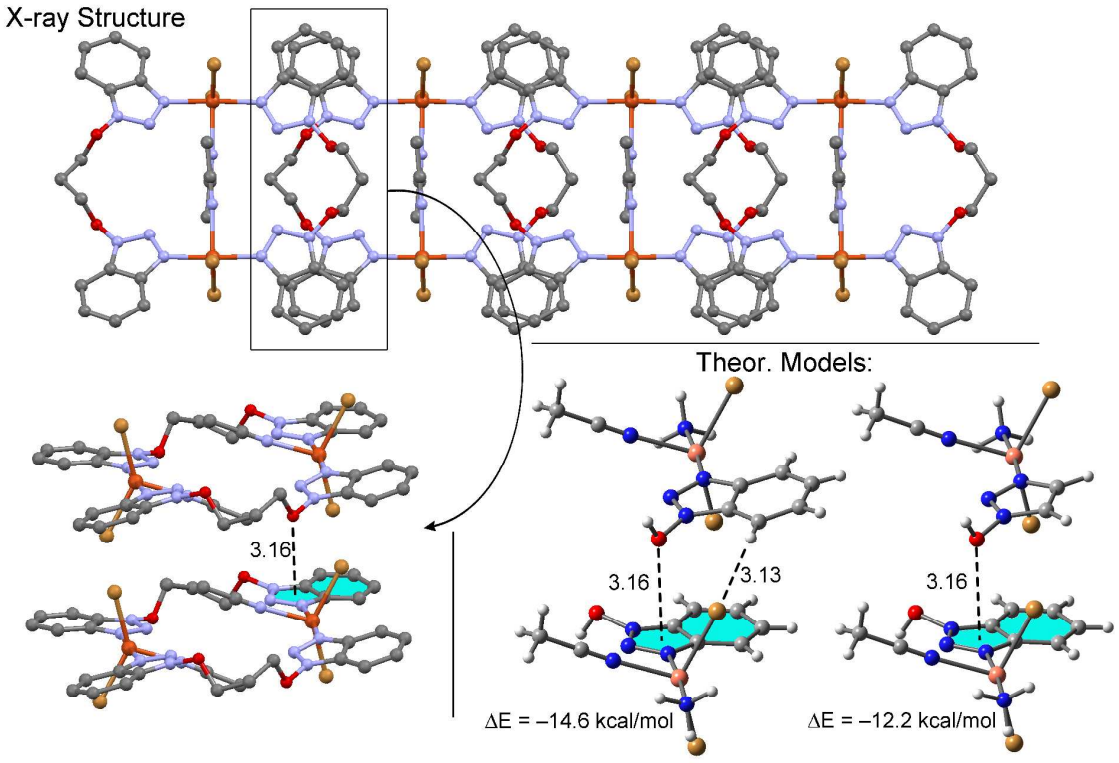

Fig. 15 X-ray fragment of compound **3** exhibiting an lp–π interaction. The theoretical models used to evaluate this interaction are also indicated. Distances in Å.

As explained above, an unprecedented and interesting C–H/σ interaction has been observed in the solid state geometry of compound **2**.[57a] In order to perform a more detailed analysis of the ability of M_2X_2 rhombus cores to participate in noncovalent interactions, we have studied the energetic and geometric features of several complexes involving σ-aromatic systems. We have used as metal centers for the central core Cu(I/II) and Hg(I/II) ions with the presence of Cl, Br, I and S acting as countercations. The *cis*-diaminoethene and oxalaldehyde ligands (L) have been chosen to complete the coordination sphere of the metal centers in the theoretical models. The σ-aromatic cores used in this study are shown in **Fig. 16.**

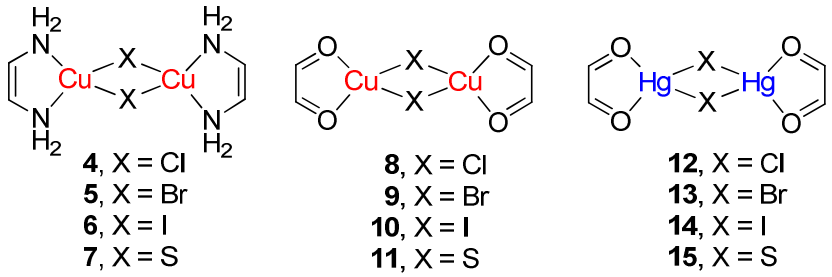

Fig. 16 Theoretical models of the σ-aromatic cores used in this study. For compound **4**–**6** and **8**–**10** we have used Cu(I) and for compounds **7** and **11** we have used Cu(II). For compound **12**–**14** we have used Hg(I) and for compound **15** we have used Hg(II).

First of all, we have analyzed the influence of the bridging ligand (X) on the aromaticity of the Cu_2X_2 core. We have selected the well-accepted Nucleus Independent Chemical Shift (NICS) as criterion for evaluating the aromatic character of different cores used in this study.[58] Recently, NICS criterion has been successfully used to characterize aromaticity in inorganic species and to classify inorganic clusters into aromatic, nonaromatic, and antiaromatic categories.[59] Moreover, the performance of this method for organic species has been demonstrated[60] and Tsipis *et al*.[61] have applied it to study cyclo-Cu_3Au_3 bimetallic clusters. In addition, NICS profiles have been recently used to classify trigonal alkaline earth metal clusters and their alkali metal salts and to

analyze the [X_2M_3] regions where the changes in aromaticity are more important.[62] Other aromaticity descriptors such as PDI,[63] FLU,[64] HOMA,[65] or ASE[66] are not straightforwardly applicable in the compounds studied in this manuscript. PDI descriptor can be used only in six-membered rings, FLU and HOMA need the use of a "fictitious" reference system that has not been defined yet for the present systems, and, finally, ASE requires the use of homodesmotic reactions that have the same number of bonds between the given atoms in each state of hybridization both in products and reactants. The necessary corrections for conjugation, hyperconjugation, etc.[67] to produce correct ASE values are still unknown in the field of inorganic compounds. Therefore, we have restricted our aromaticity study to the use of the reliable NICS index. The NICS values of complexes **4**-**11** are gathered in Table **3**.

Table 3. NICS values of the σ-aromatic Cu cores (ppm).

Complex	NICS(0)	Complex	NICS(0)
4	-14.7	**8**	-19.9
5	-21.7	**9**	-19.9
6	-24.5	**10**	-17.4
7	-27.6	**11**	-6.2

First it should be mentioned that the results gathered in Table 3 are comparable to previous studies on similar systems, for instance the NICS(0) value reported for σ-aromaticity of Cu_2O_2 based systems range from –13.3 ppm to –57.8 ppm.[57a] Some interesting conclusions can be extracted from the results of Table **3**. First, for the halogen series, the NICS values are large and negative indicating a strong σ-aromatic character. Second, when the sulfur atom is forming part of the core and, consequently, the oxidation state of the copper is 2+, the σ-aromatic character increases for the nitrogen donor ligand and decreases for the oxygen donor ligand with respect to CuI core. As a general conclusion, the NICS criterion shows that all cores have σ-

aromatic character in agreement with previous results.[57a] We have optimized different complexes involving the four membered metal cores and the C–H donor molecule HCCH, in order to evaluate the strength of the C-H/σ interaction for the different cores (see **Fig. 17**).

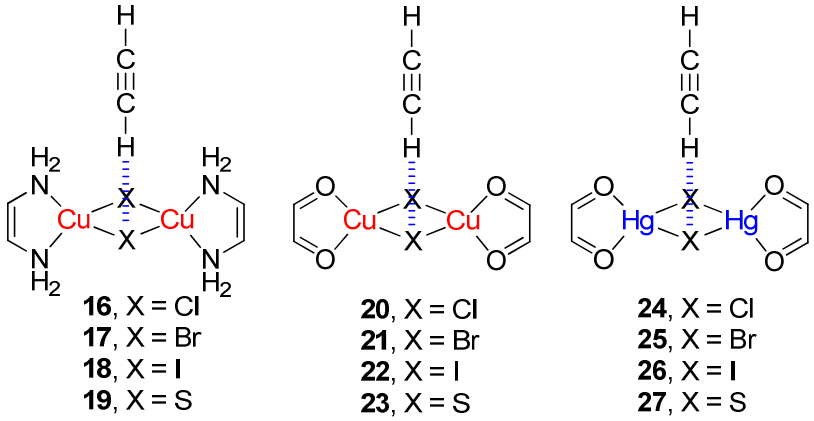

Fig. 17 C-H/σ complexes **16-27** used in this study.

In addition, we have used *cis*-diaminoethene and oxalaldehyde as ligands in order to study the influence of the donor atom of the ligand on the interaction. Moreover, to study the influence of the 2+ oxidation state of the metal centers upon the interaction energies, we have used sulfur as bridging ligand.

Table 4. Interaction energies at the BP86-D3/def2-TZVPD level of theory without and with the BSSE corrections (E and E_{BSSE}, kcal/mol) and equilibrium distances from the H atom to the ring centroid (R_e, Å).

Complex	*E*	E_{BSSE}[a]	R_e
16 (M = Cu^I, X = Cl, L = $NH_2CHCHNH_2$)	-10.4	-9.6	2.31
17 (M = Cu^I, X = Br, L = $NH_2CHCHNH_2$)	-10.4	-9.6	2.33
18 (M = Cu^I, X = I, L = $NH_2CHCHNH_2$)	-10.1	-9.6	2.37
19 (M = Cu^{II}, X = S, L = $NH_2CHCHNH_2$)	-11.4	-10.6	2.31
20 (M = Cu^I, X = Cl, L = OCHCHO)	-4.6	-3.8	2.47
21 (M = Cu^I, X = Br, L = OCHCHO)	-4.6	-3.9	2.48
22 (M = Cu^I, X = I, L = OCHCHO)	-3.4	-2.9	2.49
23 (M = Cu^{II}, X = S, L = OCHCHO)	-12.2	-11.4	2.45
24 (M = Hg^I, X = Cl, L = OCHCHO)	-2.5	-2.1	2.40
25 (M = Hg^I, X = Br, L = OCHCHO)	-2.6	-2.2	2.43
26 (M = Hg^I, X = I, L = OCHCHO)	-3.0	-2.7	2.42
27 (M = Hg^{II}, X = S, L = OCHCHO)	*Stationary point not found*		

Table **4** reports the energies and equilibrium distances corresponding to the interaction of the HCCH molecule with compounds **4-15**. From the results, some interesting conclusions can be made. Firstly, the most favorable binding energy is achieved when the sulfur acts as bridging ligand, for both N and O donor ligands (complexes **19** and **23**). This result is counterintuitive, since the presence of Cu^{II} metal centers should weaken the C–H/σ interaction due to the +2 charge of the metals. A likely explanation is that the presence of the S atoms, instead of halogen atoms, compensates this effect and favors the interaction. This issue will be further discussed below. Secondly, the strength of the C–H/σ interaction in Cu^I complexes is very similar (**16**, **17** and **18**), indicating the interaction is not influenced by the halogen atom. Conversely, the other presence of *cis*-diaminoethene or oxalaldehyde as bidentate ligand strongly influences the strength of the interaction (see Table **4**), being more favorable for the N-donor ligand. In the case of the Hg core, the interaction energies of complexes **24-26** are comparable to the corresponding

Cu complexes (**20**-**22**), indicating that the metal centers have a small influence on the interaction. For both metal cores, the energy values obtained for the three halogen atoms are very similar.

The geometries of some representative complexes are represented in **Fig. 18**. It can be observed that the planarity of the rhombus core is maintained for most complexes. In general, the bridging ligands slightly move toward the C–H donor molecule. In complex **27**, the optimization failed because of the rupture of the M_2X_2 core during the optimization process. Several attempts to minimize this complex has been unsuccessful.

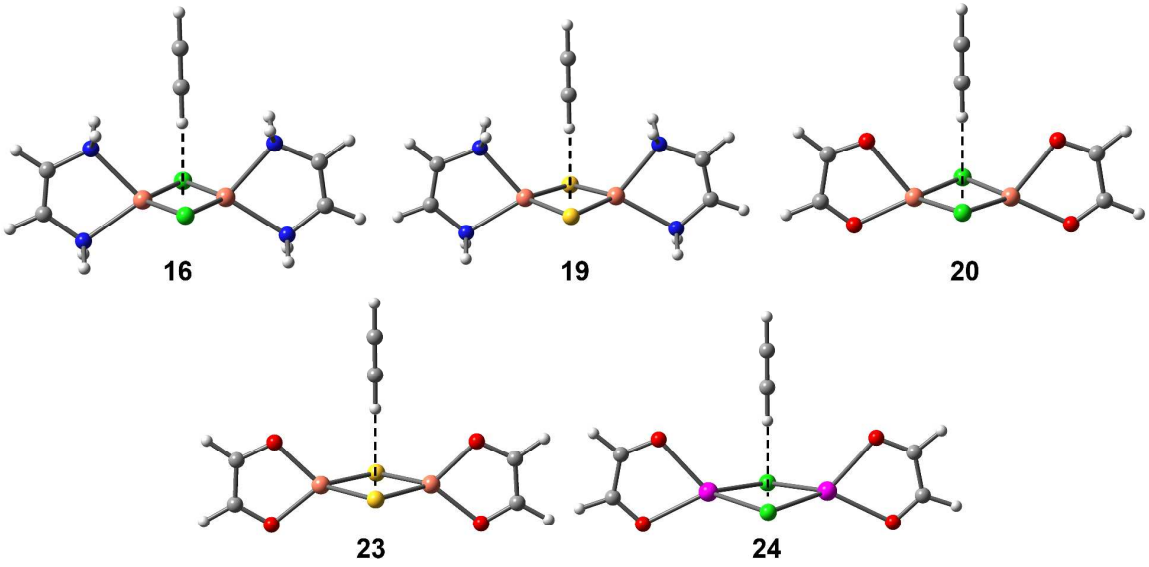

Fig. 18 C_{2v} Optimized structures of some representative C–H/σ complexes.

Finally, we have used the Bader's theory of "atoms in molecules" to further describe the noncovalent interactions presented above. In **Fig. 19** we represent the distribution of critical points and bond paths computed for complex **20** (Cu_2Cl_2 core) as a representative complex. The interaction is characterized by the presence of two bond and two ring CPs symmetrically distributed. As expected, the bond paths connect the interacting hydrogen atom with both chlorine atoms, indicating that the interaction is mainly with the bridging ligand. The Laplacian

of the charge density at the bond critical point is positive (2.00×10^{-2} a.u.) and the ellipticity is ε = 0.14 a.u. indicating that the anisotropy of the bond is very small, in contrast to the behavior previously described for complex **18** (see **Fig. 12**). The main difference between both complexes is that the bond paths connect the HCCH with the Cu metal centers in **18** and, conversely, with the Cl bridging ligands in **20**. Therefore the interaction with the *d* orbitals of the Cu metal centers results in a higher anisotropy of the noncovalent bond. The interaction is further characterized by the presence of a cage CP connecting the hydrogen atom with the center of the core. Interestingly, the presence of a cage CP is very common in π-interactions involving aromatic rings (ion– π, C-H/ π, stacking, etc.).[68]

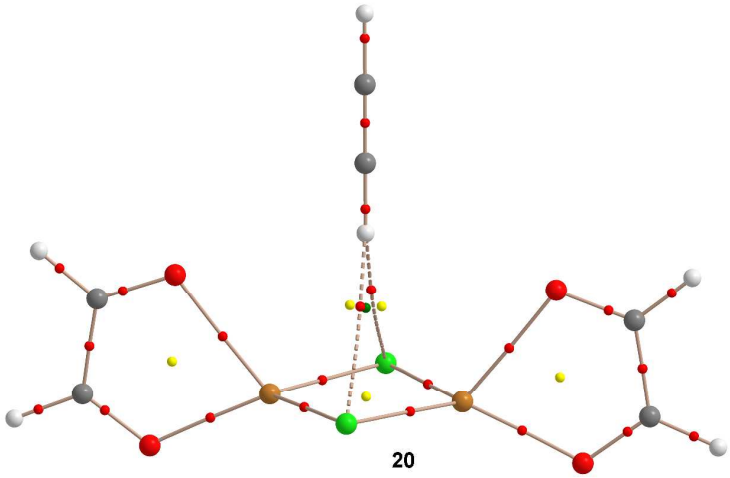

Fig. 19 AIM analysis of the C-H/σ (**20**) interaction. Bond, ring and cage critical points are represented by red, yellow and green spheres, respectively. The bond paths connecting bond critical points are also represented.

In order to complement the computational study described above characterizing the C–H/σ interaction, we have analyzed previously reported X-ray crystal structures where this interaction is present but not noticed by the original authors (See **ESI**)[69-71].

Conclusion

Novel C-H-σ supramolecular interactions involving σ-aromatic M_2X_2 cores (M=Cu, Hg; X=Cl, Br, I, S) evidenced by experimental and theoretical studies are reported for the first time. The Nucleus Independent Chemical Shift (NICs) method was used for evaluating the aromatic character of different cores in this study. The influence of the nature of metal ions, bridging atoms, oxidation states, coordination environments around the metal centers on the strength and the aromaticity of M_2X_2 cores were theoretically analyzed and explained. Analyses of supramolecular interactions reveal that C-H/σ interactions play a relevant role in the final 3D architectures of the solid state structures of several transition-metal clusters. This kind of interactions may be much more common in chemistry than one would anticipate. The advancement of the concept of aromaticity and antiaromaticity in new compounds such as polynuclear transition metal clusters is an important step in the development of a unified chemical bonding theory as well as in the comprehension of new supramolecular interactions which eventually will provide us with the ability to intelligently design new materials with desired properties. This kind of interaction is generally found in Cu_nI_n cluster with organic ligand. CuI is largely used as a catalyst in the form of powder, amorphous, nano particles in organic synthesis for C-C, C-N and C-S coupling, C-H bond activation for synthesis of interesting natural product like or pharmaceutical compounds. In most cases the reaction mechanism is still uncertain and this interaction could have a role in this processes.

The following conclusion can be drawn regarding the comprehensive theoretical study of C–H/s complexes involving different types of M_2X_2 cores: (i) for the halogen series, the NICS values are large and negative indicating a strong σ-aromatic character; (ii) with sulfur atom as a bridging atom, the σ-aromatic character increases for the nitrogen donor ligand and decreases for

the oxygen donor ligand with respect to the CuI core; (iii) the C-H/σ interaction, the most favorable binding energy, is achieved when the sulfur acts as bridging ligand, for both N and O donor ligands. For Cu^{II} metal centers, however, the C–H/σ interaction should be weakened due to the 2+ charge of the metals; (iv) the strength of the C–H/σ interaction in Cu^{I} complexes is very similar, indicating the interaction is not influenced by the halogen atom; (v) N-donor ligand is more favorable for the interaction; (vi) the interaction energies of Hg complexes are comparable to those of the corresponding Cu complexes, indicating that the metal centers have a small influence on the interaction; (vii) the planarity of the rhombus core is maintained for most complexes.

Finally, the binding ability of the 1-alkoxy-1,2,3-benzotriazole ring to establish π–π and C-H/π interactions and how its coordination to a Cu(I) and Cu(II) ions affects the strength of the aforementioned interactions have been discussed. The electron deficient triazole ring and its π-acidity increases upon coordination of the Cu ion leading to the formation of a lone pair (lp)–π interaction involving the five-membered ring of the ligand have also been analyzed. Moreover, VTM, photoluminescence and TGA studies were also carried out of the complexes.

Supporting Information

CCDC 807183, 807184, and 831721 contains the supplementary crystallographic data for **1** and **2,** and **3**, respectively. These data can be obtained free of charge via www.ccdc.cam.ac.uk or from the Cambridge Crystallographic Data Centre, 12 Union Road, Cambridge CB2 1EZ, UK; fax: (+44) 1223-336-033; or e-mail: deposit@ccdc.cam.ac.uk.

Acknowledgement

A. Sasmal gratefully acknowledges Council of Scientific and Industrial Research (CSIR), New Delhi, Govt. of India, for awarding Senior Research Fellowship (SRF) to him [CSIR Sanction No.09/096/0586/2009-EMR-I].

References

1. K. Müller-Dethlefts, P. Hobza *Chem. Rev.* **2000**, *100*, 143–167.
2. L. Pauling, M. Delbrurk, *Science*, **1940**, *92*, 77–79.
3. (a) T. J. Mooibroek, P. Gamez, J. Reedijk, *CrystEngComm*, **2008**, *10*, 1501–1515. (b) A. Frontera, *Coord. Chem. Rev*. **2013**, *257*, 1716–1727. (c) A. Frontera, P. Gamez, M. Mascal, T. J. Mooibroek, J. Reedijk *Angew. Chem., Int. Ed.* **2011**, *50*, 9564–9583
4. L. Yong, S. D. Wu, X. X. Chi *Int. J. Quant. Chem.*, **2007**, *107*, 722–728.
5. X. X. Chi, Y. Liu *Int. J. Quant. Chem.*, **2007**, *107*, 1886-1896.
6. L. Yong, X. X. Chi *J. Mol. Struct.(THEOCHEM)*, **2007**, *818*, 93-99.
7. B. B. Averkiev, A. I. Boldyrev *J. Phys. Chem. A*, **2007**, *111*, 12864-12866.
8. B. Wang, H. J. Zhai, X. Huang, L. S. Wang *J. Phys. Chem. A*, **2008**, *112*, 10962-10967.
9. H. Tanaka, S. Neukemans, E. Janssens, R. E. Silverans, P. Lievens *J. Am. Chem. Soc.*, **2003**, *125*, 2862-2863.
10. T. H□ltzl, E. Janssens, N. Veldeman, T. Veszprem, P. Lievens, M. T. Nguyen *Chem. Phys. Chem.*, **2008**, *9*, 833-838.
11. T. H□ltzl, N. Veldeman, T. Veszpremi, P. Lievens, M. T. Nguyen *Chem. Phys. Lett.*, **2009**, *469*, 304-307.
12. C. S. Wannere, C. Corminboeuf, Z. X. Wang, M. D. Wodrich, R. B. King, P. v. R. Schleyer *J. Am. Chem. Soc*., **2005**, *127*, 5701-5705.
13. Y. C. Lin, D. Sundholm, J. Juselius, L. F. Cui, X. Li, H. J. Zhai, L. S. Wang *J. Phys. Chem. A*, **2006**, *110*, 4244-4250.
14. Q. Kong, M. Chen, J. Dong, Z. Li, K. Fan, M. Zhou *J. Phys. Chem. A*, **2002**, *106*, 11709-11713.

15. C. A. Tsipis, A. C. Tsipis *J. Am. Chem. Soc.*, **2003**, *125*, 1136-1137.

16. C. A. Tsipis, E. E. Karagiannis, P. F. Kladou, A. C. Tsipis *J. Am. Chem. Soc.*, **2004**, *126*, 12916-12929.

17. C. A. Tsipis, A. C. Tsipis *J. Am. Chem. Soc.*, **2005**, *127*, 10623-10638.

18. A. C. Tsipis, A. V. Stalikas *New J. Chem.*, **2007**, *31*, 852-859.

19. X. Huang, H. J. Zhai, B. Kiran, L. S. Wang *Angew. Chem. Int. Ed.*, **2005**, *44*, 7251-7254.

20. H. J. Zhai, B. B. Averkiev, D. Y. Zubarev, L. S. Wang, A. I. Boldyrev, *Angew. Chem.Int. Ed.*, **2007**, *46*, 4277-4280.

21. H. -J. Zhai, B. Wang, X. Huang, L. S. Wang *J. Phys. Chem. A*, **2009**, *113*, 9804-9813.

22. (a) H. J. Zhai, B. Wang, X. Huang, L. S. Wang *J. Phys. Chem. A*, **2009**, *113*, 3866-3875. (b) W. -J. Chen, H. -J. Zhai, Y. -F. Zhang, X. Huang, L. S. Wang *J. Phys. Chem. A*, **2010**, *114*, 5958-5966.

23. C. Corminboeuf, P. v. R. Schleyer, R. B. King *Chem. Eur. J.*, **2007**, *13*, *978-984*.

24. R. B. King *Inorg. Chim. Acta*, **2003**, *350*, 126-130.

25. L. Alvarado-Soto, R. Ramirez-Tagle, R. Arratia-Perez, *Chem. Phys. Lett.*, **2008**, *467*, 94-96.

26. L. Alvarado-Soto, R. Ramirez-Tagle, R. Arratia-Perez *J. Phys. Chem. A*, **2009**, *113*, 1671-1673.

27. A. P. Sergeeva, A. I. Boldyrev *Comm. Inorg. Chem.*, **2010**, *31*, 2-12.

28. P. F. Weck, A. P. Sergeeva, E. Kim, A. I. Boldyrev, K. R. Czerwinski *Inorg. Chem.*, **2011**, *50*, 1039-1046.

29. L. Lin, P. Lievens, M. T. Nguyen *J. Mol. Struct. THEOCHEM*, **2010**, *943*, 23-32.

30. L. Lin, T. H□ltzl, P. Gruene, P. Claes, G. Meijer, A. Fielicke, P. Lievens, M. T. Nguyen *Chem. Phys. Chem.*, **2008**, *9*, 2471-2474.

31. S. Li, H. J. Zhai, L. S. Wang, D. A. Dixon *J. Phys. Chem. A*, **2009**, *113*, 11273-11278.

32. H. J. Zhai, L. S. Wang *Chem. Phys. Lett.*, **2010**, *500*, 185-195.

33. A. Munoz-Castro, R. Arratia-Perez *J. Phys. Chem. A*, **2010**, *114*, 5217-5223.

34. A. Munoz-Castro, D. Mac-Leod Carey, R. Arratia-Perez *J. Chem. Phys.*, **2010**, *132*, 164308.

35. A. P. Sergeeva, A. I. Boldyrev *Phys. Chem. Chem. Phys.*, **2010**, *12*, 12050-12054.

36. (a) J. -C. Guo, S. -D. Li *Eur. J. Inorg. Chem.*, **2010**, 5156-5160; (b) A. C. Tsipis, C. E. Kefalidis, C. A. Tsipis *J. Am. Chem. Soc.*, **2008**, *130*, 9144-9155.

37. W. Yamaguchi *Int. J. Quant. Chem.*, **2010**, *110*, 1086-1091.

38. A. C. Tsipis, C. E. Kefaldis, C. A. Tsipis *J. Am. Chem. Soc.*, **2007**, *129*, 13905-13922.

39. T. H□ltzl, M. T. Nguyen, T. Veszpremi *Phys. Chem. Chem. Phys.*, **2010**, *12*, 556-558.

40. A. C. Tsipis, I. G. Depastas, E. E. Karagiannis, C. A. Tsipis, *J. Comput. Chem.*, **2010**, *31*, 431-446.

41. A. C. Tsipis, C. E. Kefalidis, C. A. Tsipis *J. Am. Chem. Soc.*, **2008**, *130*, 9144-9155.

42. R. Ahlrichs, M. Bär, M. Häser, H. Horn, C. Kölmel *Chem. Phys. Lett.*, **1989**, ***162***, 165–169.

43. Gaussian 03, Revision C.01, M. J. Frisch, G. W. Trucks, H. B. Schlegel, G. E. Scuseria, M. A. Robb, J. R. Cheeseman, J. A. Montgomery, Jr., T. Vreven, K. N. Kudin, J. C. Burant, J. M. Millam, S. S. Iyengar, J. Tomasi, V. Barone, B. Mennucci, M. Cossi, G. Scalmani, N. Rega, G. A. Petersson, H. Nakatsuji, M. Hada, M. Ehara, K. Toyota, R. Fukuda, J. Hasegawa, M. Ishida, T. Nakajima, Y. Honda, O. Kitao, H. Nakai, M. Klene,

X. Li, J. E. Knox, H. P. Hratchian, J. B. Cross, V. Bakken, C. Adamo, J. Jaramillo, R. Gomperts, R. E. Stratmann, O. Yazyev, A. J. Austin, R. Cammi, C. Pomelli, J. W. Ochterski, P. Y. Ayala, K. Morokuma, G. A. Voth, P. Salvador, J. J. Dannenberg, V. G. Zakrzewski, S. Dapprich, A. D. Daniels, M. C. Strain, O. Farkas, D. K. Malick, A. D. Rabuck, K. Raghavachari, J. B. Foresman, J. V. Ortiz, Q. Cui, A. G. Baboul, S. Clifford, J. Cioslowski, B. B. Stefanov, G. Liu, A. Liashenko, P. Piskorz, I. Komaromi, R. L. Martin, D. J. Fox, T. Keith, M. A. Al-Laham, C. Y. Peng, A. Nanayakkara, M. Challacombe, P. M. W. Gill, B. Johnson, W. Chen, M. W. Wong, C. Gonzalez, and J. A. Pople, Gaussian, Inc., Wallingford CT, 2004.

44. S. B. Boys, F. Bernardy *Mol. Phys.*, 1970, **19**, 553–566.

45. R. F. W. Bader *Chem. Rev*., 1991, **91**, 893–928; AIMAll (Version 13.11.04), T. A. Keith, TK Gristmill Software, Overland Park KS, USA, 2013.

46. (a) Belletti, D, **1993**, Internal Report 1/93, Centro di Studio per la Strutturistica Diffrattometrica del CNR, Parma, Italy. (b) Bruker (**2000**, **2008**). SADABS, SMART and SAINT. Bruker AXS Inc., Madison, Wisconsin, USA. (c) A. C. T. North, D. C. Phillips, F. S. Mathews *Acta Cryst.* 1968, **A24**, 351-359. (d) A. Altomare, M. C. Burla, M. Camalli, G. L. Cascarano, C. Giacovazzo, A. Guagliardi, A. G. G. Moliterni, G. Polidori, R. Spagna *J. Appl. Cryst.* **1999**, *32*, 115-119. (e) G. M. Sheldrick, *Acta Cryst*. **2008,** *A64*, 112-122. (f) G. M. Sheldrick *SHELXTL-97*, *Program for X-Ray Crystal Structure Solution*, Göttingen (Germany): Univ. of Göttingen, **1997.** (g) L. J. Farrugia *J. Appl. Cryst.,* **1997**, *30*, 565.

47. A. W. Addison, T. N. Rao, J. Reedijk, J. V. Rijn, G. C. Verschoor *J. Chem. Soc., Dalton Trans.* **1984**, 1349-1356.

48. A. Rodriguez-Fortea, P. Alemany, S. Alvarez, E. Ruiz *Inorg. Chem.*, **2002**, *41*, 3769-3778.

49. (a) B. Scott, U. Geiser, R. D. Willett, B. Patyal, C. P. Landee, R. E. Greeney, T. Manfredini, G. C. Pellacani, A. B. Corradi, L. P. Battaglia *Inorg. Chem.* **1988**, *27*, 2454-2460. (b) G. O'Bannon, R. D. Willett *Inorg. Chim. Acta* **1981**, *53*, L131-L132. (c) G. Maass, B. Gerstein, R. D. Willett, *J. Chem. Phys.* **1967**, *46*, 401-402; (e) C. P. Landee, A. Djili, D. F. Mudgett, M. Newhall, H. Place, B. Scott, R. D. Willett *Inorg. Chem.* **1988**, *27*, 620-627. (f) D. R. Bloomquist, R. D. Willett *J. Am. Chem. Soc.* **1981**, *103*, 2615-2619. (g) R. Fletcher, J. J. Hansen, J. Livermore, R. D. Willett *Inorg. Chem.* **1983**, *22*, 330-334. (h) M. Inoue, M. Kishita, M. Kubo *Inorg. Chem.* **1967**, *6*, 900-902. (i) K. Hara, M. Inoue, S. E. Mori, M. Kubo *J. Magn. Res.* **1971**, *4*, 337-346. (j) A. Colombo, L. Menabue, A. Motori, G. C. Pellacani, W. Porzio, F. Sandrolini, R. D. Willett *Inorg. Chem.* **1985**, *24*, 2900-2905. (k) S. A. Roberts, D. R. Bloomquist, R. D. Willett, H. W. Dodgen *J. Am. Chem. Soc.* **1981**, *103*, 2603-2610.

50. (a) S. G. N. Roundhill, D. M. Roundhill, D. R. Bloomquist, C. Landee, R. D. Willett, D. M. Dooley, H. B. Gray *Inorg. Chem.* **1979**, *18*, 831-835. (b) P. Kapoor, A. P. S. Pannu, M. Sharma, M. S. Hundal, R. Kapoor, M. Corbella, N. Aliaga-Alcalde, *J. Mol. Struct*, **2010**, 981, 40-45.

51. P. C. Ford, A. Vogler *Acc. Chem. Res.* **1993**, *26*, 220-226.

52. P. C. Ford, E. Cariati, J. Bourassa *Chem. Rev.* **1999**, *99*, 3625-3647.

53. P. D. Harvey, M. Knorr *Macromol. Rapid Commun.* **2010**, *31*, 808.

54. H. N. Peindy, F. Guyon, A. Khatyr, M. Knorr, C. Strohmann *Eur. J. Inorg. Chem.* **2007**, 823.

55. H. Araki, K. Tsuge, Y. Sasaki, S. Ishizaka, N. Kitamura *Inorg. Chem.* **2005**, *44*, 9667-9675.

56. M. Vitale, C. K. Ryu, W. E. Palke, P. C. Ford *Inorg. Chem.* **1994**, *33*, 561-566

57. (a) I. Banerjee, M. Dolai, A. D. Jana, K. K. Das, M. Ali *Cryst. Eng. Comm.*, **2012**, *14*, 4972–4975. (b) M. Brookhart, M. L. H. Green, G, Parkin *Proc. Nat. Acad. Sci.* **2007**, 104, 6908–6914.

58. Z. Chen, C. S. Wannere, C. Corminboeuf, R. Puchta, P. v. R. Schleyer *Chem. Rev*., **2005**, *105*, 3842–3888.

59. J. O. C. Jiménez-Halla, E. Matito, J. Robles, M. Solà *J. Organomet. Chem*. **2006**, 691, 4359-4366.

60. (a) A. Stanger *J. Org. Chem*. **2006**, 71, 883-893. (b) A. Stanger *Chem. Eur. J*. **2006**, 12, 2745-2751.

61. C. A. Tsipis, I. G. Depastas, C. E. Kefalidis *J. Comput. Chem*. **2007**, 28, 1893-1908.

62. J. O. C. Jiménez-Halla, E. Matito, L. Blancafort, J. Robles, M. Solà *J. Comput. Chem.* **2009**, 30, 2764–2776.

63. J. Poater, X. Fradera, M. Duran, M. Solà *Chem. Eur. J*. **2003**, 9, 400-406.

64. E. Matito, M. Duran, M. Solà *J. Chem. Phys*. **2005**, 122, 014109.

65. J. Kruszewski, T. M. Krygowski *Tetrahedron Lett*. **1972**, 13, 3839-3842.

66. (a) M. K. Cyrański, *Chem. Rev*. **2005**, 105, 3773-3811; (b) W. J. Hehre, R. T. McIver, J. A. Pople, P. v. R. Schleyer *J. Am. Chem. Soc*. **1974**, 96, 7162-7163.

67. M. D. Wodrich, C. S. Wannere, Y. Mo, P. D. Jarowski, K. N. Houk, P. v. R. Schleyer *Chem. Eur. J*. **2007**, 13, 7731-7744.

68. A. Frontera, D. Quiñonero, P. M. Deyà *WIREs Comput. Mol. Sci*. **2011**, *1*, 440–459

69. I. Jes, P. Taborsky, J. Pospísil, C. Näther *Dalton Trans.*, **2007**, *22*, 2263–2270.

70. S. M. Fang, Q. Zhang, M. Hu, B. Xiao, L. M. Zhou, G. H. Sun, L. J. Gao, M. Du, C. S. Liu *Cryst. Eng. Comm.*, **2010**, 12, 2203–2212.

71. M. Knorr, F. Guyon, A. Khatyr, C. Strohmann, M. Allain, S. M. Aly, A. Lapprand, D. Fortin, P. D. Harvey *Inorg. Chem.* **2012**, 51, 9917−9934.

Table of Contents

Relevant and Unprecedented C-H/σ Supramolecular Interactions Involving σ-Aromatic M_2X_2 Cores

Ashok Sasmal[a], Antonio Bauzá[b], Antonio Frontera[b], Corrado Rizzoli[c], Cédric Desplanches[d], Loïc J. Charbonnière[d], Samiran Mitra*[a]

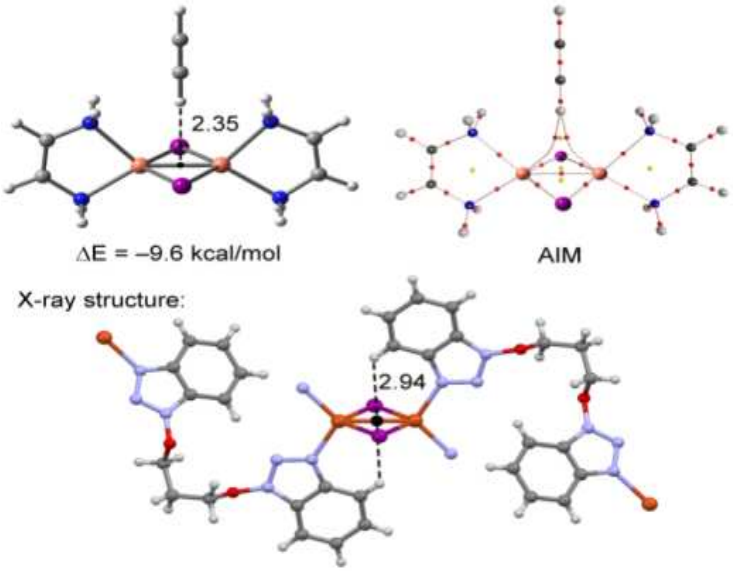

A novel C-H/σ supramolecular interaction involving σ-aromaticity M_2X_2 cores is reported for the first time. This interaction is very similar to a C-H···π interaction which has been confirmed by Bader's "atoms-in-molecules" AIM analysis.